



Article

Vegetation Stress Monitor—Assessment of Drought and Temperature-Related Effects on Vegetation in Germany Analyzing MODIS Time Series over 23 Years

Ursula Gessner ^{1,*} , Sophie Reinermann ² , Sarah Asam ¹ and Claudia Kuenzer ^{1,2}

¹ German Remote Sensing Data Center (DFD), German Aerospace Center (DLR), 82234 Wessling, Germany; sarah.asam@dlr.de (S.A.); claudia.kuenzer@dlr.de (C.K.)

² Department of Remote Sensing, Institute of Geography and Geology, University of Würzburg, 97074 Würzburg, Germany; sophie.reinermann@dlr.de

* Correspondence: ursula.gessner@dlr.de

Abstract: Over the past two decades, and particularly since 2018, Central Europe has experienced several droughts with strong impacts on ecosystems and food production. It is expected that under accelerating climate change, droughts and resulting vegetation and ecosystem stress will further increase. Against this background, there is a need for techniques and datasets that allow for monitoring of the timing, extent and effects of droughts. Vegetation indices (VIs) based on satellite Earth observation (EO) can be used to directly assess vegetation stress over large areas. Here, we use a MODIS Enhanced Vegetation Index (EVI) time series to analyze and characterize the vegetation stress on Germany's croplands and grasslands that has occurred since 2000. A special focus is put on the years from 2018 to 2022, an extraordinary 5-year period characterized by a high frequency of droughts and heat waves. The study reveals strong variations in agricultural drought patterns during the past major drought years in Germany (such as 2003 or 2018), as well as large regional differences in climate-related vegetation stress. The northern parts of Germany showed a higher tendency to be affected by drought effects, particularly after 2018. Further, correlation analyses showed a strong relationship between annual yields of maize, potatoes and winter wheat and previous vegetation stress, where the timing of strongest relationships could be related to crop-specific development stages. Our results support the potential of VI time series for robustly monitoring and predicting effects of climate-related vegetation development and agricultural yields.

Keywords: Enhanced Vegetation Index (EVI); climate impact; heat; yields; agriculture; cropland; grassland



Citation: Gessner, U.; Reinermann, S.; Asam, S.; Kuenzer, C. Vegetation Stress Monitor—Assessment of Drought and Temperature-Related Effects on Vegetation in Germany Analyzing MODIS Time Series over 23 Years. *Remote Sens.* **2023**, *15*, 5428. <https://doi.org/10.3390/rs15225428>

Academic Editors: Marguerite Madden, Alisa Coffin and Rosanna Rivero

Received: 6 September 2023

Revised: 6 November 2023

Accepted: 11 November 2023

Published: 20 November 2023



Copyright: © 2023 by the authors. Licensee MDPI, Basel, Switzerland. This article is an open access article distributed under the terms and conditions of the Creative Commons Attribution (CC BY) license (<https://creativecommons.org/licenses/by/4.0/>).

1. Introduction

Droughts pose a major threat to ecosystems and food production. They can have strong regional impacts on hydrology, soil moisture, land CO₂ uptake, vegetation condition, crop production and forestry [1–7]. For Central Europe, an increase in warm-season droughts has been observed over the past 15 years [8], and it is expected that with accelerating climate change, droughts will further increase in terms of spatial extent, duration and socio-economic impacts [9–12]. The year 2003 was characterized by exceptionally dry conditions, but particularly since 2018, Central Europe has experienced an extraordinary frequency of droughts. The 2018–2020 period was characterized by an unprecedentedly intense series of hot and dry weather conditions [11], which was again followed by droughts in 2022. It was shown for Europe that compound droughts since 2018 have resulted in an amplification of impacts via cascading or preconditioning effects [1,13] and in significant economic damages in agriculture and forestry [1,11].

Against this background, there is a need for techniques and datasets that will allow for monitoring of the timing, extent and effects of droughts. Droughts are complex phenomena that usually start with a lack of precipitation over a period of time (meteorological drought),

can subsequently develop to an inadequate availability of surface and subsurface water resources (hydrological drought) and can lead to declining soil moisture and crop failure (agricultural drought) [14]. In addition, there are impacts on ecosystem services and related feedback in natural and/or socio-economic systems (ecological drought, [15]). The notion of 'agricultural drought' is sometimes considered ambiguous, as a decline in soil moisture does not necessarily and uniformly lead to crop failure, depending on the timing, length and magnitude of soil moisture decline as well as on the present crop type [16]. Given this complexity and the different perspectives from which droughts can be viewed, it is advisable to assess droughts using different hydrological and meteorological parameters [14]. Consequently, various drought indices have been developed [17–19]. Meteorological drought is commonly monitored using indices derived from meteorological data such as the SPI (Standardized Precipitation Index, [20], applied e.g., in [21–25]) and the SPEI (Standardized Precipitation Evapotranspiration Index, [26], used e.g., in [21,27–30]). The advantage of these indices is their multi-scalar nature which enables assessment of different drought types and drought impacts on diverse hydrological systems, since the time scale over which water deficits accumulate varies strongly in different environments [28]. Similarly, the PDSI (Palmer Drought Severity Index, [31], applied e.g., in [23,32]) relies on meteorological data and is sensitive to changes in evaporative demand. Meteorological information can also be integrated with remotely sensed land surface temperature data into individual indices, e.g., in the case of the DISS (Drought Information Satellite System, [33]) index. Hydrological droughts can be assessed based on reservoir levels and runoff or stream-flow indices (e.g., [34]). Agricultural droughts can be investigated based on soil moisture, e.g., [6,35,36], or by directly analyzing vegetation stress. For the latter, remote sensing time series techniques can be used to monitor vegetation conditions during droughts over large areas. From an agricultural and ecosystem perspective, the main advantage of such Earth Observation (EO)-based assessments of vegetation is that they can provide information not only on singular aspects of drought (e.g., rainfall or soil moisture deficit, low water levels), but on the integrated effect that past and recent rainfall and soil moisture deficits actually have on vegetation by also considering the present vegetation's capacity to cope with it. In the literature, several remote sensing-based indices have been used for vegetation stress and drought detection, including the VCI (Vegetation Condition Index, [37]), the VHI (Vegetation Health Index, [38]), the TCI (Temperature Condition Index, [38]), further (derivatives of) vegetation indices (VIs) such as the NDVI (Normalized Difference Vegetation Index), the EVI (Enhanced Vegetation Index) and others (e.g., [1,16,27–29,39–42]), the NDDI (Normalized Difference Drought Index [43]) and FAPAR (Fraction of Absorbed Photosynthetically Active Radiation, e.g., [24,25,44,45]). Several studies further combine remote sensing-based indices of vegetation with indices of soil moisture and meteorological and/or hydrological drought, e.g., [1,24,25], amongst others.

Earlier research has analyzed how such EO-based vegetation parameters, but also meteorological variables and soil moisture, correlate with agricultural yields in Central Europe [21,46] and Germany [47–51]. The vegetation parameters from EO used in these studies (VCI, VHI, TCI and NDVI) showed correlations with winter wheat and maize yields, but with strong regional, crop-specific, and index- or sensor-related differences in correlation strengths and in periods of highest correlations. Most of the studies (except for [47]) consider only one crop type when assessing the relevance of EO-based indices, and to our knowledge, the relationship of crop yields and deviations of EVI has not yet been tested for Germany.

This study aims to assess and characterize the vegetation stress on Germany's cropland and grassland that has occurred since 2000, with a special focus on the years between 2018 and 2022, which represent an extraordinary 5-year period containing four particularly hot and dry years. Because our intent was to assess vegetation stress directly in this study, we decided to use a pure vegetation parameter that does not include measurements of potential drivers of vegetation stress such as temperature or moisture, as is the case for, for example, TCI and VHI. We analyze time series of 250 m MODIS (Moderate Resolution

Imaging Spectroradiometer) EVI (Enhanced Vegetation Index), an index whose potential to successfully capture agricultural vegetation characteristics has been repeatedly demonstrated (e.g., [52–54]). With its temporal coverage of more than 23 years, near-daily repeat cycle and comparably high spatial resolution of up to 250 m, MODIS provides a unique dataset for long-term vegetation studies. MODIS EVI was preferred over MODIS NDVI due to its sensitivity to variations in vegetation, even in growing phases with dense vegetation cover [55]. Even though there are further MODIS-based standard products with vegetation variables such as FAPAR (fraction of absorbed photosynthetically active radiation) or LAI (leaf area index), their spatial resolution of 500 m is not as well suited as the higher resolution (250 m) EVI for capturing the relatively small-scale agricultural structures in Germany. We follow the MODIS EVI-based approach that was used by [42] in a study assessing the drought effects of the years from 2000 to 2018. We further develop and adapt the approach, now operated as the Vegetation Stress Monitor, and then re-process and update the vegetation stress time series for Germany for the period from 2000 to 2022. As different vegetation types can show very different responses to drought and extraordinary temperature conditions, we sub-differentiate between vegetation stress on croplands and grasslands in our analyses. The time series of the Vegetation Stress Monitor is presented and interpreted in the context of agricultural drought for all of Germany and for seven counties that were selected to represent typical cropland and grassland areas in the study region. Finally, we correlate the 23 years of monthly MODIS-based EVI deviations to annual yield statistics of important crop types at the county level. For this purpose, we select crop types with very different cropping calendars: maize, potatoes and winter wheat. We discuss the identified relationships in the context of crop phenology and demonstrate the applicability of the Vegetation Stress Monitor information for topics of societal relevance. The main goals of this study are to:

- Provide an improved and updated time series of monthly vegetation stress for Germany spanning the years between 2000 and 2022.
- Enhance our understanding of drought- and temperature-related patterns of vegetation stress in Germany with a particular focus on spatio-temporal differences and on the droughts that happened from 2018 to 2022 compared to previous years.
- Quantify the relationship between vegetation stress and yields for important crop types in Germany to provide a better understanding of which periods of vegetation stress throughout the growing season are most relevant and where in Germany such effects are most prominent.

Compared to [42], the underlying methodology is slightly improved (see Section 4.1), and the time series of vegetation stress is reprocessed and now also includes recent years up to 2022. The major difference from [42], however, is the detailed interpretation of vegetation stress that has occurred since 2018, its comparison to the drought year 2003, the discussion of regional differences between major German cropland and grassland areas, and the quantitative crop-specific analysis of relationships between within-season, EVI-based vegetation stress and agricultural yields. Both the detailed presentation and characterization of EVI-based seasonal vegetation stress over Germany from 2000 to 2022 and its quantitative comparison with yields for important crop types in Germany have to our knowledge not been published before.

2. Study Area

2.1. Geographic Characteristics

The presented analysis focuses on Germany, covering an area of 357.592 km². The country is located in the temperate climate zone with Atlantic influence in the northwest and more continental conditions towards the east. Mean precipitation patterns in Germany are shown in Figure 1B. Precipitation levels are below 550 mm in large parts of Eastern Germany and rise up to more than 1000 mm in the low mountain ranges and to more than 3000 mm in the Alps [56]. Annual mean and maximum temperatures (Figure 1C) are comparably low in the mountain ranges and towards the coast in the north, while

particularly high temperatures are found in the more continental east of Germany as well as in the river valleys of the Rhine and the Main. In the coldest month of the winter season (January), typical mean temperatures range from $-10\text{ }^{\circ}\text{C}$ in the alpine regions to $3.5\text{ }^{\circ}\text{C}$ in the northwest, whereas in the warmest month of the summer season (July), mean temperatures range from $3.2\text{ }^{\circ}\text{C}$ in the Alps and $20.4\text{ }^{\circ}\text{C}$ in the east as well as in the regions of Rhine and Main [56]. Around one half of Germany's land area is used for agriculture (50.5%, Figure 1). Of this agricultural area, 70% is cropland, and 29% is permanent grassland [57,58]. The most common crops grown in the study region are wheat, maize, barley, rapeseed and rye [58]. From an administrative perspective, Germany consists of 16 federal states (*Bundesländer*, NUTS-1, Figure 1B). As the three federal states of Hamburg, Berlin and Bremen are dominated by urban areas and have only minor vegetated land cover, we did not consider them in the statistical analyses of our results. The federal states are subdivided into 400 counties (*Landkreise* and *kreisfreie Städte*, NUTS-3).

While the major part of this study analyses the whole of Germany, we focused on seven selected counties (Figure 1A) for a more detailed investigation of temporal patterns. These focus counties represent the range of typical major cropland and grassland regions of Germany (Table 1). We selected five cropland-dominated counties, as the typical cropland regions are diverse and widely spread over Germany while major grassland regions mainly exist in the pre-alpine (south) and coastal (north) areas of Germany, represented by two focus counties in this study.

Table 1. Overview of the focus counties of this study. In the abbreviations used for the focus counties, “C” stands for crop-dominated counties, while “G” indicates grassland-dominated agriculture.

Focus County	Mean Temperature ($^{\circ}\text{C}$) Average of 1991–2020 [59]	Maximum July Temperature ($^{\circ}\text{C}$) Average of 1991–2020 [60]	Annual Rainfall (mm) Average of 1991–2020 [61]	Muencheberger Soil Quality Rating (min–max (mean)) ¹ [62,63]
C1—Demmin	9.1	23.4	592	27–69 (56)
C2—Steinfurt	10.2	23.9	784	19–78 (61)
C3—Soemmerda	9.6	24.9	542	46–98 (89)
C4—Wuerzburg	9.7	25.2	658	29–77 (59)
C5—Rottal–Inn	9.1	24.7	875	57–77 (69)
G1—Cuxhaven	9.7	22.5	832	19–78 (61)
G2—Ostallgaeu	7.6	22.2	1314	59–77 (73)

¹ <35: extremely low, 35–50: very low, 50–60: low, 60–70: average, 70–85: high, >85: very high.

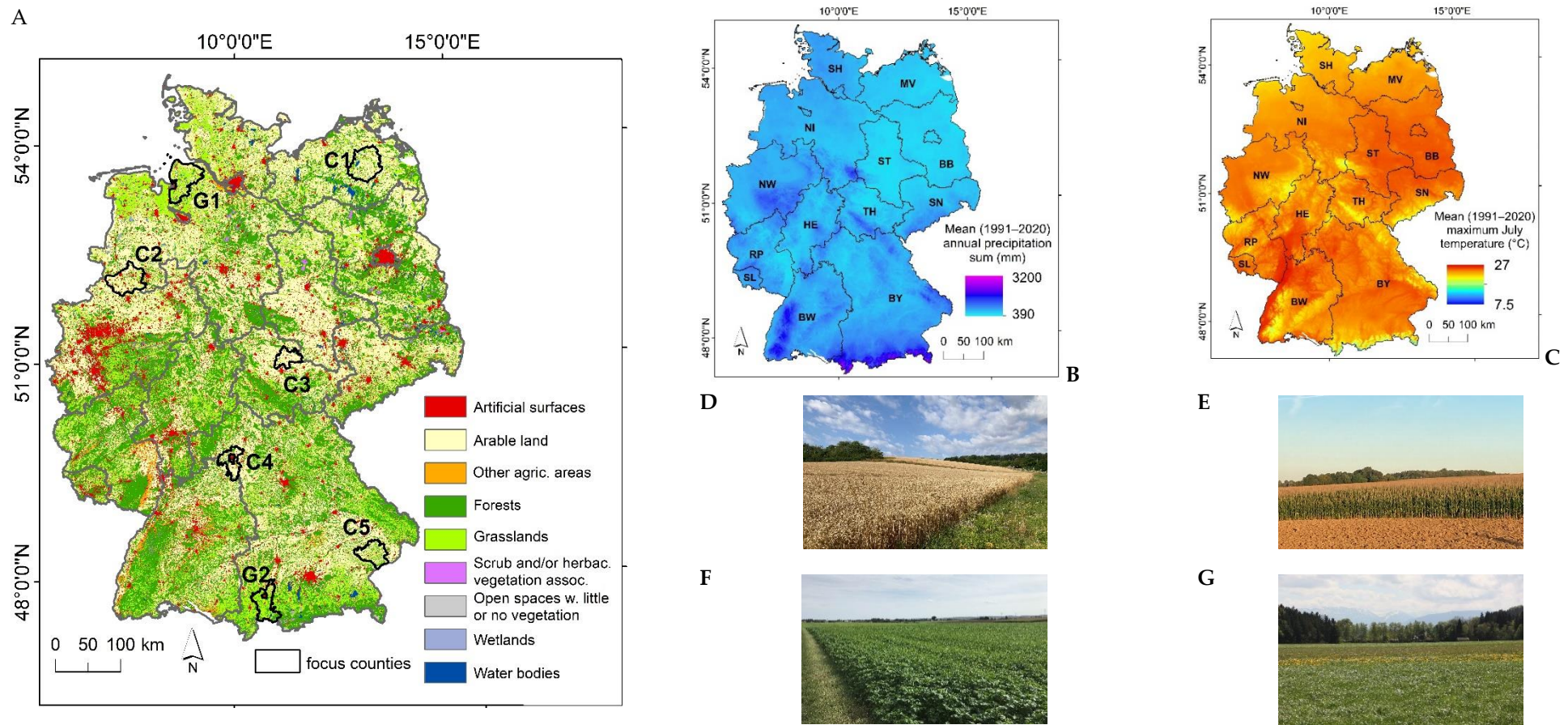


Figure 1. Germany's land cover (A, based on CORINE 2018 [64]), gridded station data (1 km × 1 km) of average precipitation sums (B, DWD Climate Data Center (CDC) [61]), gridded station data (1 km × 1 km) of average daily maximum temperatures for July (C, DWD CDC) and pictures of typical agricultural areas (D—winter wheat, E—maize, F—potatoes, G—grassland; pictures taken by U. Gessner, A. Schucknecht and J. Meier). Grey (A) and black (B,C) lines demark the borders of non-urban federal states (BB—Brandenburg, BW—Baden Wurttemberg, BY—Bavaria, HE—Hesse, MV—Mecklenburg–Western Pomerania, NI—Lower Saxony, NW—North Rhine Westphalia, RP—Rhineland Palatinate, SH—Schleswig–Holstein, SL—Saarland, SN—Saxony, ST—Saxony–Anhalt, TH—Thuringia). Black lines in A show the focus counties of this study (C1—Demmin, C2—Steinfurt, C3—Soemmerda, C4—Wuerzburg, C5—Rottal-Inn, G1 Cuxhaven, G2—Ostallgaeu).

2.2. Dry and Hot Years 2018–2022

For a better understanding of the focus years between 2018 and 2022, the following subsection will give background information on the reported meteorological conditions and agricultural yield fluctuations in the study region during this period.

In Germany—with the exception of the year 2021—the past five years (2018–2022) were at the same time exceptionally warm and dry. With average annual temperatures of 10.5 °C, 10.3 °C, 10.4 °C and 10.5 °C, the four years 2018, 2019, 2020 and 2022 were amongst the five warmest years since the beginning of regular records in 1881 and experienced negative rainfall anomalies relative to the period between 1881 and 2022 [65].

However, also in 2021, average annual temperatures over Germany (9.2 °C) were higher than the long-term average temperatures of 8.2 °C that were recorded for the reference period of 1961 to 1990 [66]. Of the past five years, 2018 was the most extreme, with the highest annual average temperature and the fourth lowest precipitation level since 1881 in Germany; in summer and autumn 2018, only 50% of the average precipitation was recorded [67]. Figure 2 gives an overview of deviations in precipitation (left) and temperature (right) compared to the period of 1961–1990 for spring (March, April, May), summer (June, July, August) and autumn (September, October, November), for each federal state. The seasonal precipitation maps (Figure 2 left) show that in the past five years, above-average rainfall at larger extents occurred only in autumn 2019 (northern Germany), in autumn 2022 (southern Germany) and in summer 2021 (most parts of Germany). Positive temperature deviations (Figure 2 right, red) highlight the fact that not only annual but also seasonal averages for all seasons with vegetation activity were above the values of the reference period 1961–1990, with the only exception being spring 2021 where below-average temperatures caused a late onset of spring.

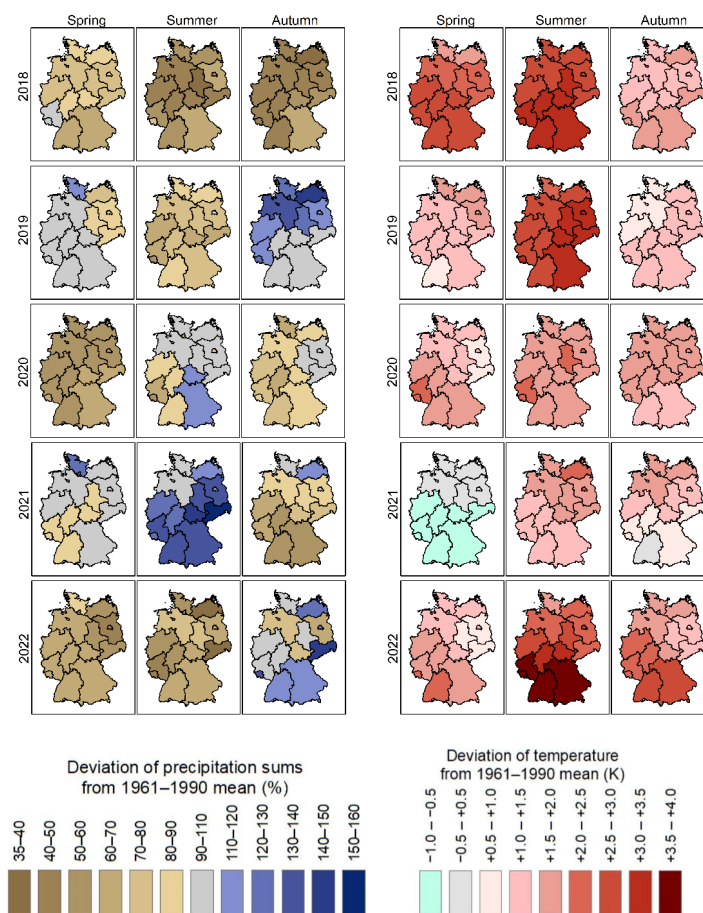


Figure 2. Precipitation sums (left) and mean temperature (right) in spring (MAM), summer (JJA) and autumn (SON) 2018–2022 compared to long-term (1961–1990) averages. Data were extracted from

climate status reports from the German Weather Service [65–69], attached to federal state boundaries and mapped using the GIS (Geographical Information System).

The hot and dry conditions in 2018–2020 and 2022 affected agricultural yields, but spatial and temporal patterns are quite complex. Figure 3 shows the fluctuations of selected crops with different cropping cycles and differing agrometeorological requirements as extracted from yield statistics of the German Federal Statistical Office and the German Federal Ministry of Food and Agriculture [70,71].

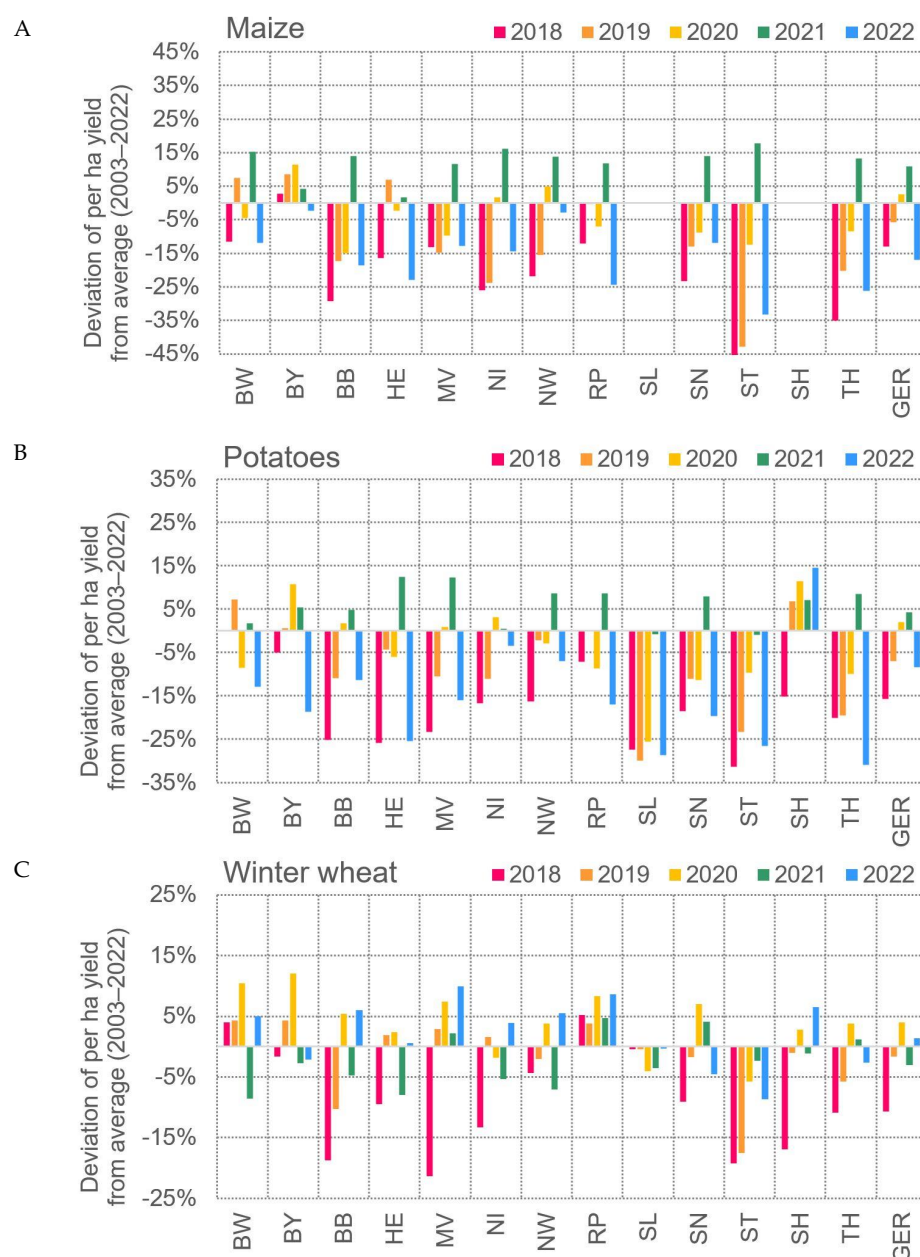


Figure 3. Deviation of yields per hectare for selected crop types in Germany and in German federal states for the years from 2018 to 2021 compared to multi-year averages (2003–2022): (A) maize; (B) potatoes; (C) winter wheat. BB—Brandenburg, BW—Baden Wurttemberg, BY—Bavaria, HE—Hesse, MV—Mecklenburg–Western Pomerania, NI—Lower Saxony, NW—North Rhine Westphalia, RP—Rhineland Palatinate, SH—Schleswig–Holstein, SL—Saarland, SN—Saxony, ST—Saxony–Anhalt, TH—Thuringia; GER—Germany. Data source: Official statistical data based on farm surveys, published by the German Federal Statistical Office and the German Federal Ministry of Food and Agriculture in [70,71].

In 2018, yields per ha were considerably low for almost all crop types and federal states. Exceptions were the States NW, RP, SL, BW and BY, located in the south, southwest and west, where winter wheat yields were around average. Per-hectare yields of potatoes and maize were clearly below average for all states in 2018, except for the south (BY and BW). Also, in 2019, widespread yield deficits occurred but were not as strong as in 2018. Yields were around (+/− 5%) or below average for all considered crop types and regions, except for potatoes and maize in BW and for maize in BY. In 2020, per-hectare yield of winter wheat were around (+/− 5%) or higher than normal for all of Germany. Yields for potatoes were mixed over Germany and mainly not more than 15% below average for maize, except for BY, where maize yields were 10% above average. 2021 was a good-to-normal year for potatoes and maize all over Germany. Yields of winter wheat were mixed, but negative anomalies did not exceed 10% in any federal state. In 2022, yields of winter wheat were around (+/− 5%) or above average for all states except for ST. In contrast, potato yields were clearly below average for most regions. Maize yields were slightly (2–3%) below average in BY and NW but clearly below average for all other States in Germany.

3. Data

3.1. Satellite and Land Cover

The Vegetation Stress Monitor uses 250 m, 16-day composites of MODIS Terra EVI (MOD13Q1, v061 [72] provided by GEE) as an indicator for vegetation condition. The presented results are based on a 22-year time series of MOD13Q1 EVI spanning the period from 2000 to 2022. Due to the predominant dormancy of Central European vegetation during winter, the focus of the Vegetation Stress Monitor is on MODIS data for spring, summer and autumn, while the winter months December, January and February are excluded.

CORINE Land Cover (CLC) map products [73] with a spatial resolution of 100 m were used for excluding land cover change related effects on vegetation and for analyzing land cover-specific vegetation stress. For this purpose, the CLC map 2012 (covering the period from 2011 to 2012, which is centrally located in our study period) and the CORINE Land Cover Change Layers (CHA 2000–2006, 2006–2012 and 2012–2018) version 2020_20u1 were used.

3.2. Yield Statistics

For analyzing the relationship between EVI-based vegetation stress and agricultural yields, we selected crop types that are highly relevant in Germany and that show different phenologies and cropping calendars: winter wheat (being the most widespread crop type in Germany, covering 2.89 million hectares, and a typical representative of winter cereals), maize (being the second most widespread crop type in Germany, covering 2.49 million hectares, a cereal with later sowing and later harvest), and potatoes (which cover only 0.26 million hectares, but which are an important staple crop that can be considerably affected by water deficits) (all numbers from [74] for the year 2022). Annual statistics on yields for these crop types were taken from the regional database of the German Federal and States Statistical Offices [75]. The data were downloaded at the level of counties for the years 2000 to 2022 in values of dt (decitonnes, 1 dt = 100 kg) yield per hectare. As described in [76], these data have been collected in the framework of the German-wide ‘crop and farm reporting for crops and grassland’ (*Ernte- und Betriebsberichterstattung für Feldfrüchte und Grünland*) conducted by the German federal states and coordinated by the Federal Statistical Office of Germany (Destatis). Yield information is collected via country-wide uniform questionnaires. These are answered by yield reporters for farms that are selected systematically by the statistical offices of the federal states in a non-random approach [76].

4. Methods

4.1. Vegetation Stress Assessment

The original methodology of the Vegetation Stress Monitor was published in [42]. In the present study, the methodological workflow is described, with a focus on several improved details. An overview of the workflow is shown in Figure 4. Vegetation conditions are assessed based on the deviations of MODIS EVI from its long-term average at 16-day intervals. Compared to the previous version [42], where 19 years of MODIS data were available, the presented analyses now rely on a prolonged time series of 22-years (2000–2021) for calculating the long-term median, and deviations are calculated until 2022. MODIS data of low quality (e.g., cloud-affected and marginal data) is excluded by selecting only those pixels for further analyses which are labeled as best quality (class 0) in the MOD13Q1 “250 m 16 days pixel reliability” quality layer. Furthermore, non-vegetated areas are excluded by masking pixels with EVI values below zero and by masking all pixels assigned as non-vegetated land cover classes (e.g., “urban” and “water”) in the CLC product 2012. Finally, all pixels that show changes in the CLC change layers are excluded from further processing. In this study, different from [42], the application of the change layers CHA 2000–2006 and CHA 2006–2012 were complemented by the newest change layer CHA 2012–2018. This ensures that land cover or land use changes are not misinterpreted as vegetation stress and do not affect the long-term mean.

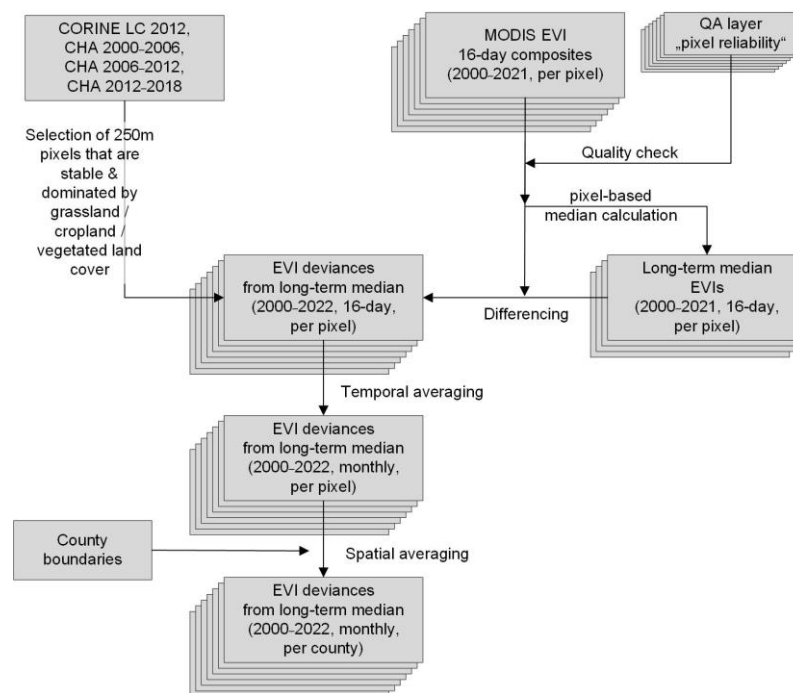


Figure 4. Overview over the methodological workflow.

The 22-year median (2000–2021) is calculated for each MOD13Q1 16-day composite. Then, the EVI difference between each original 16-day EVI composite and the 22-year median EVI of the same composite period is calculated. This results in a 16-day composite time series of EVI deviations from their long-term average. This 16-day time series is temporally aggregated to monthly and annual intervals in order to minimize outlier effects. The monthly datasets are calculated by averaging pairs of those two 16-day EVI deviations which have the longest overlapping period with the respective month, as shown in Table S1 of the supplementary material. Negative EVI deviations are considered an indicator of vegetation stress.

The resulting monthly EVI deviations are stratified by three (groups of) land cover/use classes: cropland classes, grassland classes and all vegetated land cover classes, based on the

100 m CLC product. The CLC level 2 class 21 “arable land” is used for identifying cropland, and the CLC level 3 classes 231 “pastures” and 321 “natural grasslands” are merged to identify grassland areas. Further, as described above, only areas that showed stable land cover throughout the period of investigation—as indicated in the three most recent Corine change layers—were considered. Subsequently, the sub-pixel fraction of each MODIS 250 m pixel with respect to the considered higher resolution CLC classes is calculated, and only relatively pure MODIS pixels with at least 75% sub-pixel coverage of grassland, cropland and vegetated classes, respectively, are considered for further processing.

The monthly and annual EVI deviations for cropland, grassland, and all vegetated classes are averaged over all German counties and federal states by considering only those MODIS pixels where the respective land use/cover class is predominant (75% sub-pixel coverage). To avoid unrepresentative values, average EVI deviations are not calculated for administrative units that comprise less than 10 valid pixels of the class under consideration. All described processing is conducted on the Google Earth Engine platform (<https://earthengine.google.com/>, last accessed on 1 September 2023) [77].

4.2. Correlation Analyses

The relationship between EVI deviations and agricultural yields for the period 2000–2022 was assessed by calculating Spearman correlation coefficients per county and crop type. In this correlation analysis, the annual yield statistics of maize, potatoes and winter wheat were correlated with the county-averaged EVI deviations of each month individually but considering only those months in which the respective crop type is usually cultivated. Months prior to planting and months after harvest were not considered. In case less than 80% of the annual data pairs (deviations of monthly EVI and crop yield) contained valid data in a county, the result for the respective county was labeled “not sufficient data”. This happened due to missing statistical yield information for several counties and crop types but also (to minor extent) due to missing vegetation stress data.

5. Results

5.1. Vegetation Stress Detection in Germany for 2000–2022

The spatial patterns of vegetation stress over Germany as mapped via the Vegetation Stress Monitor based on MODIS EVI time series are shown in Figure 5 on county level for all vegetated land cover classes averaged over June, July, August and September (JJAS) for 2000 until 2022. The well-known drought years 2003 and 2018 can be easily depicted. In 2003, most parts of the country were affected by strong negative deviations of JJAS vegetation activity with the strongest effects in the central and southern parts. In 2018, the likewise strong negative deviations were mainly found in the central and northern parts of Germany, while in this case, the south was affected to a smaller degree.

This is also reflected in Figure 6A, which shows that JJAS vegetation stress was stronger in the northern parts of Germany in 2018 compared to 2003, while in southern Germany, vegetation stress was more pronounced in 2003, compared to 2018. The vegetation stress observed for summer was slightly more widespread for 2003 (365 counties, corresponding to ca. 90% of Germany) compared to 2018 (295 counties, corresponding to ca. 80% of Germany; Figures 5 and 6B). Vegetation stress was also detected in other years but with lower intensities and to lesser extents (e.g., 2000: north and east, 2001: south, 2006: north and west, 2007: west, 2011: central west, 2015: south). However, it also becomes obvious that an accumulation of years with strong negative deviations of vegetation activity can be observed after 2018. Except for the year 2021 with a relatively wet summer (for rainfall deviations see Figure 2), all years since 2018 showed moderate to strong vegetation stress in different regions of Germany (2019: east and north, 2020: central west, 2022: center, west, and north).

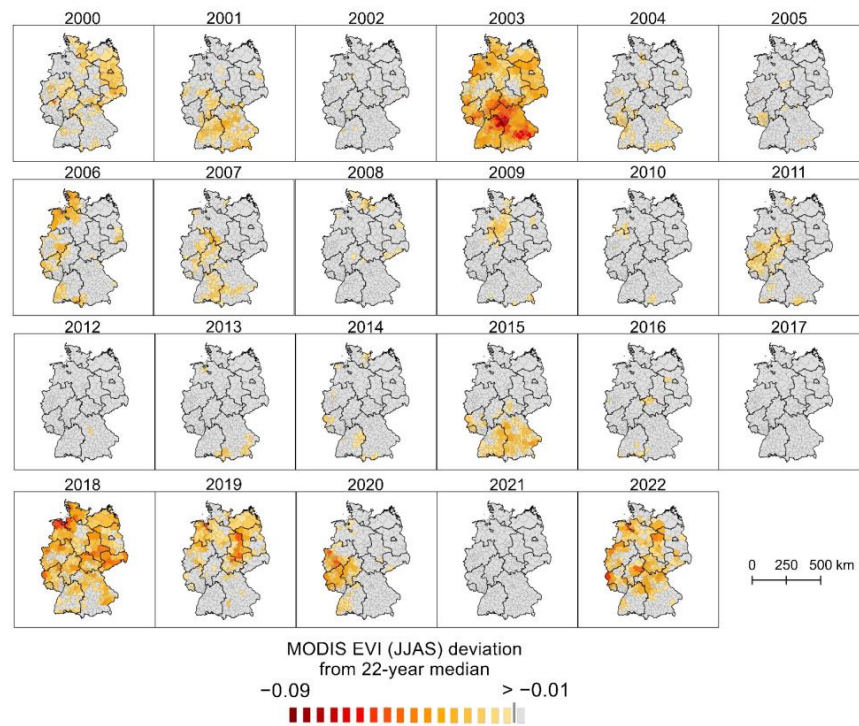


Figure 5. Annual vegetation stress averaged over June–September (JJAS) and over each county for the years 2000–2018 as derived by the Vegetation Stress Monitor from MODIS EVI time series.

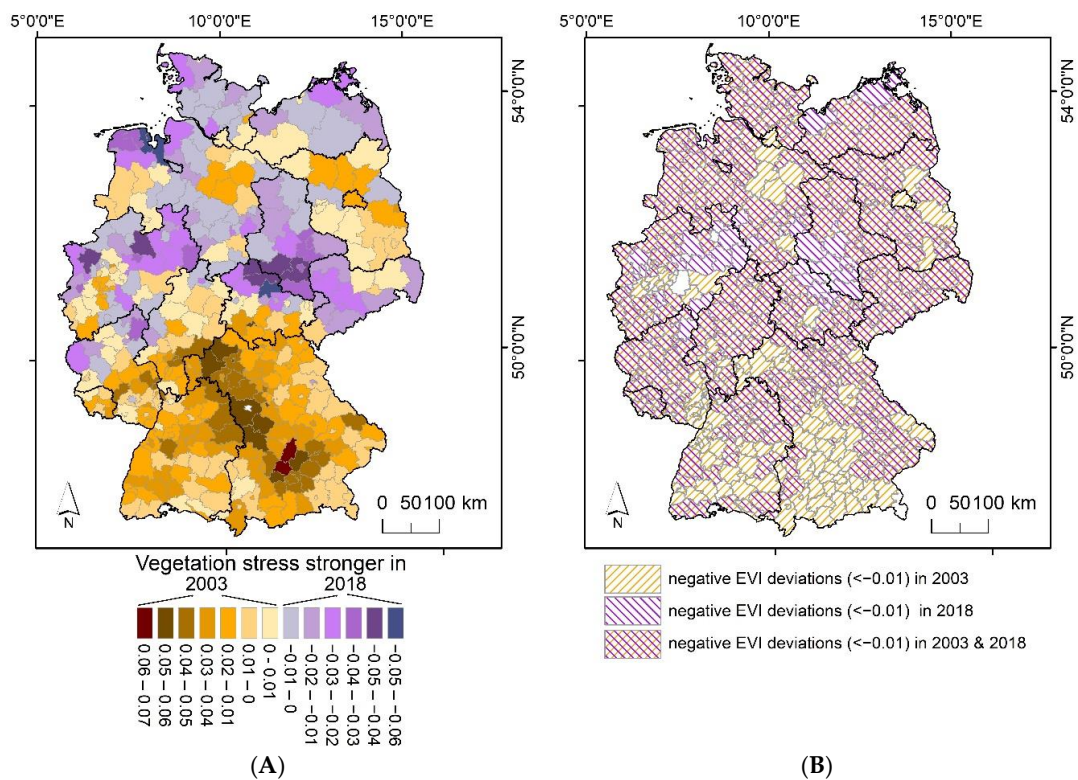


Figure 6. Comparison of vegetation stress observed for 2003 and 2018 during the summer months JJAS: (A) shows the difference between EVI JJAS deviations of 2018 and 2003. Positive values indicate stronger negative EVI deviations in 2003, and negative values indicate stronger negative EVI values in 2018; (B) shows the counties that were characterized by negative EVI deviations (<−0.01) in the years 2003, 2018 and both 2003 and 2018.

The monthly patterns of deviations in vegetation activity from 2000 to 2022 are illustrated in Figure 7 for selected cropland focus counties and in Figure 8 for selected grassland focus counties (see Figure 1A). The selected focus counties represent the range of typical major cropland and grassland regions of Germany as described in Section 2.1. By comparing the long-term temporal patterns of vegetation stress for these selected focus areas, we intend to discover if there are major differences or similarities within the major cropland regions and within the major grassland regions, but also between grasslands and croplands. For the focus counties C1–C5, which are dominated by cropland use, we show EVI deviations averaged only over predominant cropland pixels within this county, while for the focus counties G1 and G2, which are dominated by grassland, we show EVI deviations averaged only over predominated grassland pixels.

The monthly time series of cropland focus counties (Figure 7) show that the general accumulation of strong vegetation stress since 2018—which has been observed for the summer months in Germany (Figure 5)—has complex regional and seasonal patterns. In the county of Demmin (C1), the negative deviations of cropland vegetation activity in the summer months June and July of 2018, 2019 and 2022 stand out for the study period since 2000. Negative EVI deviations in spring (March–May) were much stronger in other years (e.g., in 2003, 2010, 2011 and 2016), but not as pronounced for the years 2018–2022.

This pattern is similar for cropland in the county of Soemmerda (C3), which is located about 400 km to the South. Here also, June and July 2018, 2019 and 2022 show particularly negative deviations when compared to other years since 2000. In contrast, negative spring deviations cannot be observed for these years and were much more pronounced, e.g., in 2006, 2010 and 2013 and strongest in the drought year 2003.

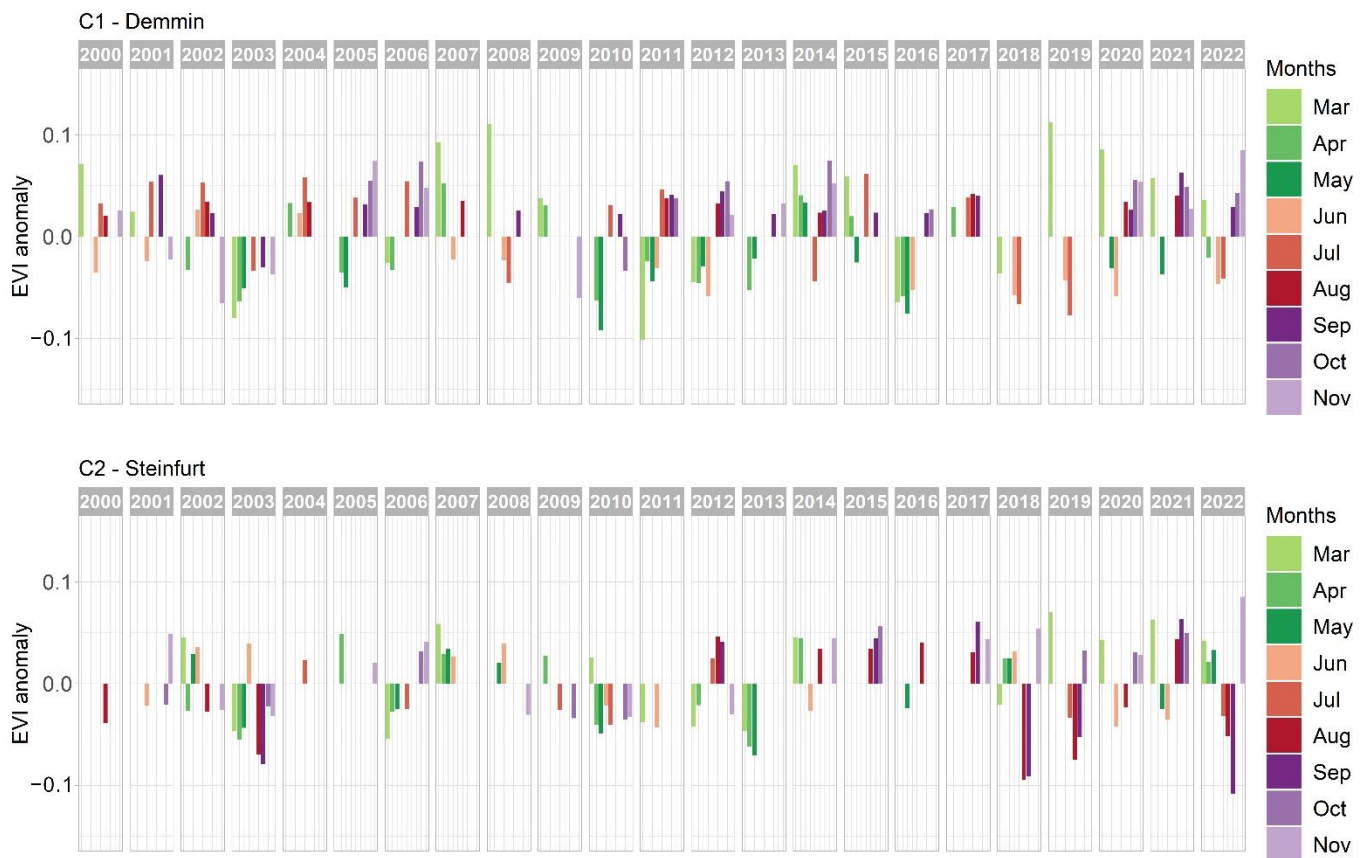


Figure 7. Cont.



Figure 7. Monthly deviations of MODIS EVI 2000–2022 averaged over all cropland pixels in the focus counties C1–C5. The location of the focus counties is shown in Figure 1A.

For the county of Steinfurt (C2), the EVI deviations over cropland for July/August to September for 2018, 2019 and 2022 are among the strongest negative deviations over the complete time series, but this is not the case for other months of the growing season. Similarly strong negative deviations for late summer/early autumn can be observed in the drought year 2003. In this year, however, the spring months also showed negative EVI deviations which are, after 2013, the second strongest ones observed since 2000.

In the county of Würzburg (C4), negative deviations in late summer and autumn 2018, for 2022 and 2003 are of similar magnitudes and are lower than in any other year since 2000. In 2003, however, negative deviations were also found for spring and early summer, so 2003 is the year where vegetation stress was strongest and most long-lasting

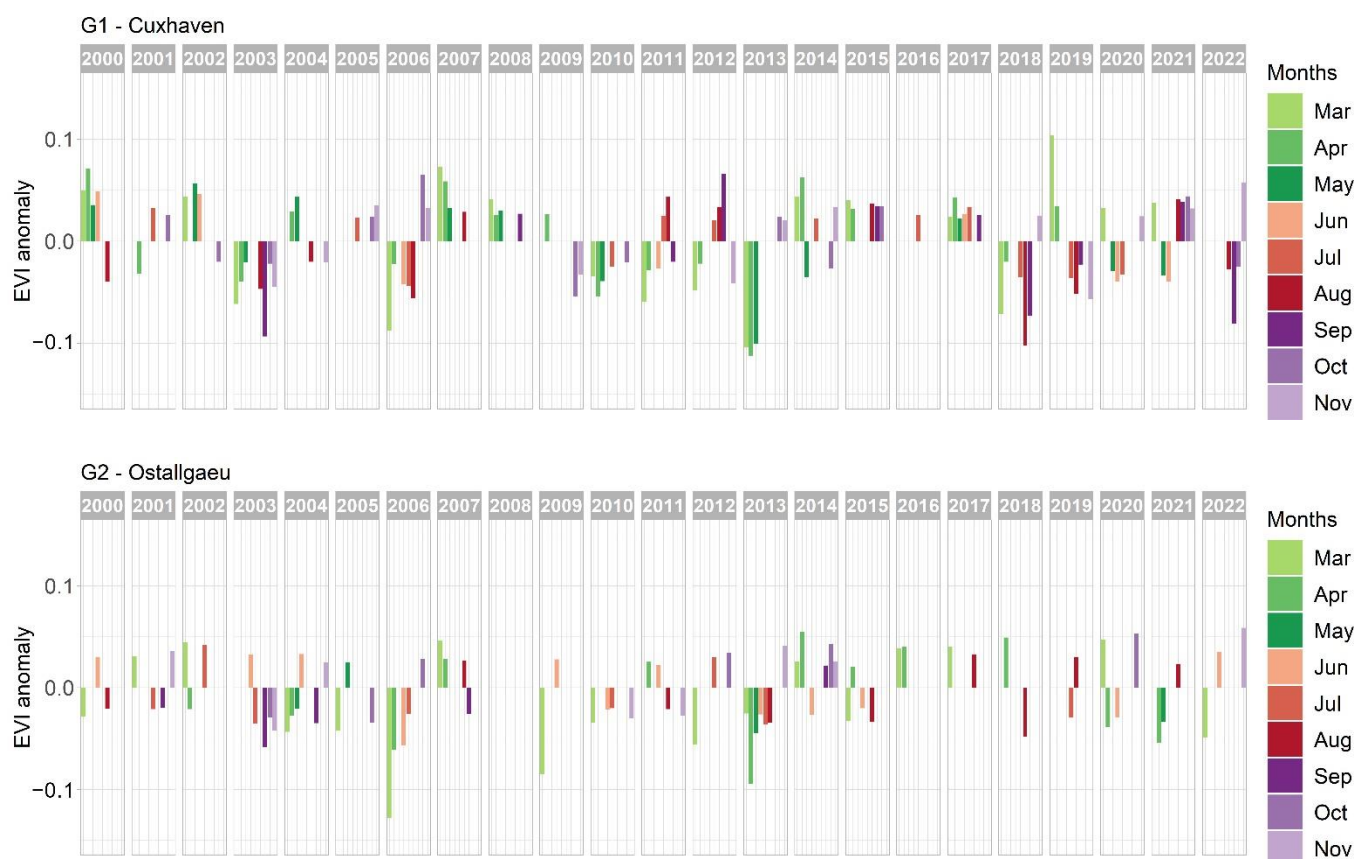


Figure 8. Monthly deviations of MODIS EVI 2000–2022 averaged over all grassland pixels in the focus counties G1 and G2. The location of the focus counties is shown in Figure 1A.

The croplands of the county Rottal–Inn (C5) do not show any unique behavior since 2018, with only relatively weak negative late summer/early autumn deviations in 2018 and 2022, which could be found at similar to even stronger magnitudes also in 2015. More pronounced are negative EVI deviations for 2003, a year which was additionally affected by strong negative deviations in spring, i.e., by constant negative EVI deviations throughout the vegetation period.

Figure 8 shows that for the grasslands of the county Cuxhaven in northern Germany (G1), negative deviations in late summer/early autumn 2018, 2019 and 2022 were similar to those of 2003. Spring 2018 showed similar, but not as long-lasting, negative deviations as spring 2003, but the strongest negative spring deviations in this county were detected for the year 2013.

The grasslands in the county of Ostallgaeu (G2) are relatively stable and show the least pronounced EVI deviations among all focus counties. No exceptional behavior for the years since 2018 can be observed. The comparably strongest negative deviations are observed in the spring months of 2006, 2009 and 2013. For 2003, negative deviations are observed mainly in autumn.

5.2. Detected Vegetation Stress Characteristics for Germany in 2018–2022

As illustrated above, years with strong negative deviations of vegetation activity have occurred more frequently after 2018 compared to 2000–2017 (Figure 5), but with regional and seasonal variations (Figure 7). We therefore have a closer look at the monthly vegetation stress situation between 2018 and 2022. Figure 9 shows vegetation stress for spring, summer and autumn months (Mar–Nov) in 2018–2022 as indicated by the Vegetation Stress Monitor. Please note that Figure 9 shows more months than were included in Figure 5 (there: June–September). The maps display EVI deviations for all vegetated land cover classes at the

level of the German counties. Vegetation stress maps for grassland and cropland can be found in the supplementary material (Figures S1 and S2), which generally exhibit quite similar overall spatial and temporal patterns. Figure 9 shows distinct phases of vegetation stress (marked by black boxes in Figure 9) for all years, however with varying magnitudes, duration, and timing. The longest and most pronounced phase of vegetation stress is found in 2018 lasting from June to October (Figure 9, box A). EVI deviations were observed between June and July mainly in the northeast, expanding to the northwest in August and September, and weakening in October. Southern Germany (i.e., the southern parts of BY and BW) was less affected compared to the rest of Germany in 2018. In 2019, vegetation stress was detected between June and September (Figure 9, box B) but at lower magnitudes compared to 2018 and spatially more limited. Negative deviations of EVI occurred in the northeast in June, in the northern half of Germany in July, and they were attenuating and retracting in August/September. In 2020 (Figure 9, box C), subtle signs of vegetation stress are detectable in northeastern Germany in May, while in June, large areas all over Germany were affected. From July to September, slightly higher intensities of vegetation stress were identified for the western center of Germany, while the situation attenuated for the rest of the country. In 2021, EVI deviations did not show any sign of vegetation stress for the summer and autumn months. However, in spring 2021 (April to May), strong negative deviations were observed for most parts of Germany, which attenuated in June (Figure 9, box D). In 2022 (Figure 9, box E), relatively weak vegetation stress was identified in June for the northeast, shifting to central and southern Germany in July and August. In September 2022, relatively high levels of vegetation stress were observed for the northern half of Germany with a focus on the northwest, while the southern part of Germany (southern parts of BY and BW) were less affected.

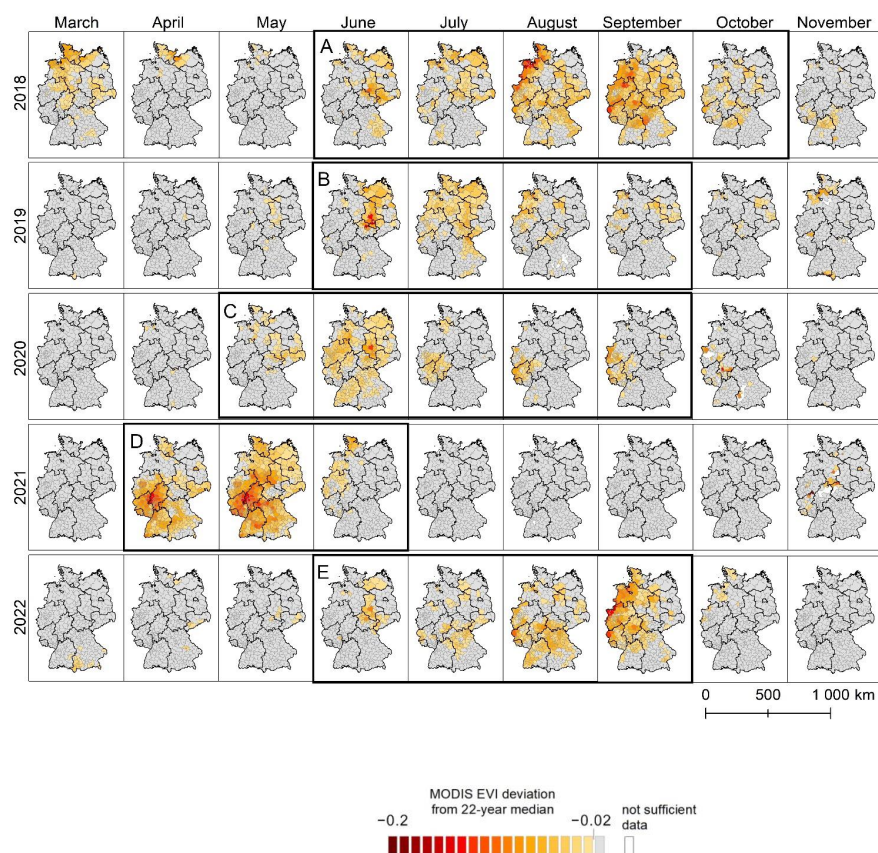


Figure 9. Monthly (Mar–Nov) maps of vegetation stress for all vegetated land cover types as indicated by MODIS EVI deviations for 2018–2022 at county level. Respective maps for cropland and grassland can be found in the supplementary material (Figures S1 and S2). Identified phases of distinct vegetation stress (A–E) are marked by black boxes.

5.3. Relationship of MODIS-Based Vegetation Stress and Agricultural Yields

Figure 10 shows the strength of the relationship between monthly EVI deviations and yields for silage maize, potatoes and winter wheat. March and September/October are not considered for maize/potatoes and winter wheat, respectively, as the selected crop types are not cultivated during these months. Grey areas indicate counties where the correlation tests revealed insignificant correlations with a 90% confidence interval. White areas are counties where we did not perform any correlation due to low data availability.

For silage maize, significant correlations were found mainly in July to September. They stretch over counties in northeastern and northern Germany in June, and expand in August to most of the country, except for the southern fringes. Significant correlations between EVI deviations and potato yields were mainly found in July–September with a peak in August. Even though the data availability for potato yield statistics is quite scattered over Germany (see white counties in line 2 of Figure 10), it can be seen that strong correlations were found for northern and eastern Germany in July and for most parts of the country in August, attenuating in September. Unlike maize and potatoes, strong correlations for winter wheat can be found in the early season (March–April). These however concentrate on eastern and southern Germany and cannot be found in the north and west.

6. Discussion

6.1. Long-Term Patterns of Vegetation Stress and the Particular Situation since 2018

The analysis of vegetation stress patterns over Germany shows that drought effects on vegetation are characterized by strong variations in space and time for both grassland and cropland areas. The time series of selected focus counties illustrate this fact exemplarily (Figures 7 and 8). The drought year 2003 was characterized by clear and relatively constant long-lasting vegetation stress for all focus counties except for the two counties in eastern Germany, Demmin (C1), where the negative deviations are not as strong, and Soemmerda (C3), where no negative deviations were detected for summer and autumn. Likewise, in both mentioned regions, topsoil moisture deficits of 2003 were not pronounced compared to other parts of the country, according to [78]. Our analyses reveal vegetation stress in 2018 for all focus counties except for Ostallgaeu (G2) and not as strong effects for Demmin (C1). The negative EVI deviations mainly occurred in summer and autumn 2018, but in most cases not in spring. For the southern focus counties of Ostallgaeu (G2) and Rottal–Inn (C5), vegetation stress in 2003 was much more pronounced than in 2018, which is in line with the comparably low summer rainfall deficits in the southernmost part of Germany in 2018. Vegetation stress at very low magnitudes was found for regions with very high annual precipitation such as G2 (Ostallgaeu, Table 1), combined with average/high soil quality (Table 1). Here, negative deviations of EVI were detectable in 2003—a year in which also southern Germany was affected by rainfall deficits and even more strongly by heat waves—but here, vegetation stress was not as strong as for the other focus counties. No clear negative effect can be observed for 2018 in G2. This indicates that this region, which is a typical example of the German pre-alpine region, was not clearly water-limited, even in extreme drought years. This assumption is supported, e.g., by [48], who revealed that heat stress can affect all of Germany, while the southernmost parts of the country are largely exempt from yield-affecting (water-related) drought stress. In contrast, in the grasslands of the focus county Cuxhaven (G1), with lower average precipitation sums (Table 1), water limitation seems to play a bigger role. Here, grasslands experienced more frequent months of negative EVI deviation, and clear vegetation stress can be observed for both 2003 and 2018.

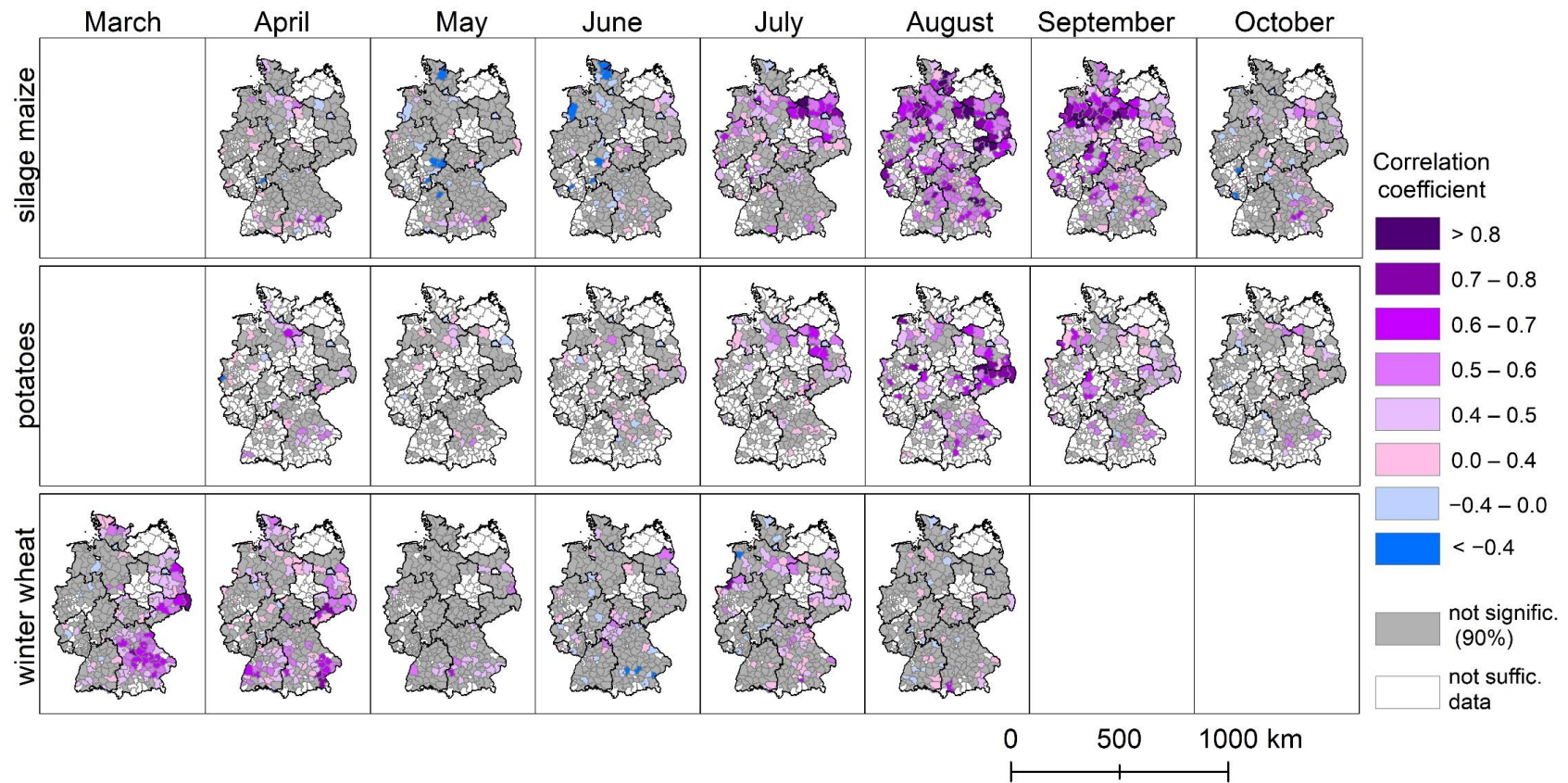


Figure 10. Correlation (Spearman's) between monthly (March–October) MODIS EVI deviations and annual yields of silage maize, potatoes and winter wheat based on county-level data for 2000–2022.

When considering Germany as a whole, the vegetation stress observed for summer (JJAS) was slightly more widespread for 2003 compared to 2018 (Figures 5 and 6). Vegetation stress during the summer months of these extreme drought years was stronger in the northern parts of Germany in 2018 compared to 2003, while in southern Germany, vegetation stress was more pronounced in 2003, compared to 2018. This observation matches with meteorological data from the German Weather Service that shows that the southern part of Germany experienced similar/only slightly higher summer precipitation and considerably higher summer temperatures in 2003, compared to 2018 [56]. The northern part of Germany, in contrast, experienced lower rainfall amounts and similar summer temperatures in 2018 compared to 2003 [56]. Also, when regarding drought intensities and magnitudes as derived from topsoil moisture data modeled by UFZ (Helmholtz-Zentrum für Umweltforschung) [78], the drought was stronger in large parts of southern Germany in 2003 and stronger in northern Germany in 2018, but overall, topsoil drought conditions (intensity and magnitude) were reported to be more widespread in 2018 [78]. While 2003 was a relatively isolated drought year, the year 2018 was the start of a period where vegetation stress areas occurred frequently, which is unique within the period of investigation. There are studies that deduced, in the case of the years 2018 and 2019, that compound drought years have amplified impacts as ecological and agricultural systems are already weakened from previous drought conditions [1,11,13]. Based on this assumption and the spatial patterns of vegetation stress detected in the presented study, such amplifying effects could be particularly relevant for the northern part of Germany where vegetation stress was observed for 2018 and 2019 consecutively.

6.2. Vegetation Stress and Yields

We found strong correlations between EVI-based monthly deviations and annual yields for silage maize, potatoes and winter wheat. There are clear differences in correlation between crop types and regions. For silage maize and potatoes, which are both planted comparably late in April and early May, correlations to vegetation stress are most prominent (strength and extent) in August. Maize yields showed stronger correlations than winter wheat and potatoes. Stronger correlations for maize than for winter wheat were also found for southern Germany (BY) by [47]. For maize, large areas with significant correlations to vegetation stress were found from July to September with highest correlation coefficients in August of up to 0.88. In this period, maize is in its flowering and milk-ripe stages, which are known to be the stages where maize is most sensitive to water deficits [79,80]. A study that correlated VCI and maize yields, [21] also found the strongest correlations for August, with similar spatial patterns, and similar but slightly higher maximum correlation coefficients (0.93). However, in this case, differing periods of investigation and correlation methods hamper a direct comparison of correlation strengths. In a study that analyzed the relationship between soil moisture, precipitation and temperature with maize yields, the strongest correlations were found for a slightly earlier period (June to August) [50] than found here, which could be explained by a lagged response of vegetation stress compared to meteorological variables and soil moisture. Further, we found a tendency towards higher correlation coefficients between vegetation stress and maize yields in the north of Germany compared to the south.

For potatoes, larger areas of strong correlations to vegetation stress are found after July, which means after canopy closure, which usually takes place in June. The higher water demands towards the later growth stages of potatoes might play a role in this observation. Between July and September, significant correlations are found for almost all counties with sufficient data availability, for at least one of the months, and with the highest correlation coefficients in the east of Germany. However, it has to be noted that the data availability for potato yield statistics is much more scattered than for maize and winter wheat, and that there is a lack of other studies on potatoes to be compared with our results.

The spatial and temporal correlation patterns for winter wheat are considerably different compared to potatoes and maize. Winter wheat, which is planted in autumn, shows

strong and widespread correlations in March (tillering phase) for northern, northeastern and southeastern Germany with a maximum correlation coefficient of 0.78, and in April (stem elongation phase) for northern, northeastern, southeastern and southwestern Germany with a maximum correlation coefficient of 0.77. This time falls into growth stages of wheat that are most sensitive to droughts [81,82]. During the tillering phase, drought most severely affects the tiller number per plant, and during the stem elongation phase, drought affects plant height [82]. Significant correlations are, however, not found in this period for large parts of the central west of Germany. High correlations for early spring (end of February to beginning of April) MODIS NDVI were also found by [46] on a national scale for Germany. The results of [49] in contrast—based on 4 km AVHRR vegetation health indices and selected farms and counties in eastern Germany—showed highest correlations with winter wheat yields for later months (April–July). Even though our analyses also showed a secondary peak of correlations in July, there are clear differences between the findings of [49] and our results as well as those of [46]. This disagreement is most likely caused by differing EO sensors and their spatial resolutions (4 km AVHRR vs. 250 m MODIS) as well as by the focus of [49] on selected farms and counties for which, to larger parts, statistical yield information was not available in our dataset. In their analysis, [51] identified highest correlations of soil moisture in March with winter wheat yields, which also fits our results, especially when considering a temporal lag between soil moisture deficits and vegetation stress. In contrast, [47] found only low correlations between their EO-based crop-specific drought indices and winter wheat yield in Germany. When comparing this finding to the results presented here, the reason for these low correlations becomes obvious: in [47], crop-specific drought indices for winter wheat were based on the months May–July but did not include information from March and April, which are here shown to be most relevant for winter wheat yields in large parts of Germany.

6.3. Strengths and Limitations

In agricultural remote sensing studies, EVI is the second most frequently used multi-spectral VI after NDVI [83]. MODIS EVI is sensitive to temporal variations in vegetation and biophysical parameters, even in areas of dense vegetation cover [55], and its capability to successfully capture vegetation characteristics in agricultural landscapes has been repeatedly demonstrated, e.g., [54,84–86]. However, monitoring approaches using multispectral VIs such as EVI have certain limitations due to factors such as the influence of soil color and canopy shadows. In the context of this study, it also has to be noted that EVI is not sensitive to vegetation condition as soon as cereals reduce their chlorophyll contents during later growth stages prior to harvest. Analyzing EVI deviations from long-term medians can be a robust alternative to drought indices such as VCI, depending on study region and application. While VCI values strongly depend on the minimum and maximum value of NDVI that occurred (once) during the period of observation, the approach presented here relates the current EVI value to all values of the historic time series by considering the more robust long-term median EVI. This is particularly relevant when the time series analyzed is not too long, when it potentially does not contain representative low or high states of the considered VI, and when there are remaining atmospheric effects in the dataset which generally decrease VI values. It however has to be considered that in our approach, vegetation classes that show stronger natural inter-annual variations are generally showing higher vegetation stress values than stable ones. This has to be considered when comparing the magnitude of vegetation stress among different vegetation or land cover types.

The interpretation and discussion of our results focuses on climate-related effects on vegetation stress. It should, however, be noted that not only climatic influences can lead to stress in vegetation. Biotic factors such as agricultural pests and diseases can principally cause vegetation stress and crop failure or develop as cascading effects resulting from unfavorable climatic conditions [87,88]. In our study region, this could be the case occasionally and in smaller regions, but at the spatial scale of our investigation, such causes

can be considered secondary and masked by climatic effects. However, this aspect could play a bigger role in future under further accelerating climatic change.

As MODIS is currently reaching the end of its lifetime, it can be expected that a continuation of the presented analyses after 2022 will lead to increasingly unreliable results. For future years, the approach will thus require an adaptation to newer missions such as VIIRS (Visible Infrared Imaging Radiometer Suite). The usage of vegetation indices show certain advantages in this regard, as they can be cross-calibrated to produce harmonized VI time series across different sensors [55,89] which could ensure continuity of long-term monitoring of climate-related vegetation stress. EVI is operationally produced from VIIRS data [90], and proved to be a reliable continuation of the MODIS mission [91]. To account for possible systematic errors in the VI time series across sensors due to differences in sensor and platform characteristics, harmonization between MODIS and VIIRS products is necessary [92].

7. Conclusions

In this study, the Vegetation Stress Monitor is used for assessing vegetation stress on Germany's cropland and grassland since 2000, with a special focus on the years 2018–2022. This MODIS-based approach is a further development of the workflow published by [42] which focuses on monthly, land cover specific deviations of MODIS-EVI from the long-term median. We present vegetation stress time series for 2000–2022 for all of Germany and for seven counties that were selected to represent typical cropland and grassland areas in Germany. Further, we correlate the monthly vegetation stress data with 23 years of annual yield statistics for three important crops in Germany. The results show that major drought- but also temperature-related effects on vegetation are well captured in the EVI-based dataset. It enables the monitoring of onset and duration of vegetation stress at monthly intervals. Strong regional differences of drought- and heat-related vegetation stress could be observed within major cropland and grassland regions of Germany. While the patterns of vegetation stress vary strongly from year to year, the northern parts of Germany showed a higher tendency to be affected by drought effects, particularly after 2018. In grasslands in the south, measurable vegetation stress turned out to hardly occur, even in extreme drought years. When comparing 2003 and 2018—two years of extreme heat and drought—we found that vegetation stress observed in summer (JJAS) was slightly more widespread in 2003. In the northern parts of Germany, summer (JJAS) vegetation stress was stronger in 2018 than in 2003, while in southern Germany, vegetation stress was more pronounced in 2003 compared to 2018. Further, we found strong correlations between the EVI-based monthly deviations and annual yields for silage maize, potatoes and winter wheat in Germany. Clear differences in correlation between crop types and regions are shown which can be largely explained by the crop-specific sensitivities to drought and heat during specific cultivation periods and growth stages.

The analyses revealed the potential of the Vegetation Stress Monitor to capture climate-related vegetation stress and to support the within-season prediction of agricultural yields. The delineated dataset of crop-specific vegetation response to past drought events could contribute to drought hazard mapping in the context of drought risk assessment and to the development of adaptation measures. Our results hence show the applicability of the Vegetation Stress Monitor to delineate relevant information for topics of societal relevance. For an improved understanding of the effects of meteorological and soil moisture related droughts on vegetation stress, future analyses could focus on identifying underlying drivers using multivariate regression (e.g., [93]) or machine learning algorithms such gradient boosting (e.g., [94–97]). For enabling the continuation of the Vegetation Stress Monitor beyond the lifetime of the MODIS mission, further work will need to focus on the harmonization of MODIS EVI with the VIIRS-based EVI product.

Supplementary Materials: The following supporting information can be downloaded at: <https://www.mdpi.com/article/10.3390/rs15225428/s1>, Figure S1: Monthly (March–November) maps of vegetation stress for grassland as indicated by MODIS-EVI deviations for 2018–2022 at county level; Figure S2: Monthly (March–November) maps of vegetation stress for cropland as indicated by MODIS-EVI deviations for 2018–2022 at county level; Table S1 Indication of the two 16-day composites used to calculate monthly EVI deviations.

Author Contributions: Conceptualization, U.G., S.R. and S.A.; methodology, S.R., U.G. and S.A.; software, S.R. and U.G.; formal analysis, U.G.; writing—original draft preparation, U.G.; writing—review and editing, S.R., S.A. and C.K. All authors have read and agreed to the published version of the manuscript.

Funding: This research was partly funded by Helmholtz-Gemeinschaft Deutscher Forschungszentren (HGF) through the Helmholtz Klimainitiative Climate Adaptation and Mitigation, Cluster II (HI-CAM) project and through internal DLR funds.

Data Availability Statement: The vegetation stress data presented in this study are available on request from the corresponding author. The data will be made available in near future in a publicly accessible repository (<https://geoservice.dlr.de/web/>. last accessed on 1 September 2023).

Acknowledgments: We gratefully acknowledge the anonymous reviewers for constructive comments for improvement of the manuscript. We would like to thank the DWD (Deutscher Wetterdienst) for providing meteorological data, and the statistical offices of Germany and of German federal states (Statistische Ämter des Bundes und der Länder, Destatis) for providing yield statistics. Finally, we would like to thank Jonas Meier and Anne Schucknecht for providing pictures for Figure 1.

Conflicts of Interest: The authors declare no conflict of interest. The funders had no role in the design of the study; in the collection, analyses, or interpretation of data; in the writing of the manuscript; or in the decision to publish the results.

References

1. Conradt, T.; Engelhardt, H.; Menz, C.; Vicente-Serrano, S.M.; Farizo, B.A.; Pena-Angulo, D.; Dominguez-Castro, F.; Eklundh, L.; Jin, H.; Boincean, B.; et al. Cross-sectoral impacts of the 2018–2019 Central European drought and climate resilience in the German part of the Elbe River basin. *Reg. Environ. Chang.* **2023**, *23*, 32. [[CrossRef](#)] [[PubMed](#)]
2. Thonfeld, F.; Gessner, U.; Holzwarth, S.; Kriese, J.; da Ponte, E.; Huth, J.; Kuenzer, C. A First Assessment of Canopy Cover Loss in Germany's Forests after the 2018–2020 Drought Years. *Remote Sens.* **2022**, *14*, 562. [[CrossRef](#)]
3. Boergens, E.; Güntner, A.; Dobslaw, H.; Dahle, C. Quantifying the Central European Droughts in 2018 and 2019 With GRACE Follow-On. *Geophys. Res. Lett.* **2020**, *47*, e2020GL087285. [[CrossRef](#)]
4. Buras, A.; Rammig, A.; Zang, C.S. The European Forest Condition Monitor: Using Remotely Sensed Forest Greenness to Identify Hot Spots of Forest Decline. *Front. Plant Sci.* **2021**, *12*, 689220. [[CrossRef](#)] [[PubMed](#)]
5. Orth, R.; Zscheischler, J.; Mahecha, M.D.; Reichstein, M. Contrasting biophysical and societal impacts of hydro-meteorological extremes. *Environ. Res. Lett.* **2022**, *17*, 014044. [[CrossRef](#)]
6. Boeing, F.; Rakovec, O.; Kumar, R.; Samaniego, L.; Schrön, M.; Hildebrandt, A.; Rebmann, C.; Thober, S.; Müller, S.; Zacharias, S.; et al. High-resolution drought simulations and comparison to soil moisture observations in Germany. *Hydrol. Earth Syst. Sci.* **2022**, *26*, 5137–5161. [[CrossRef](#)]
7. Bastos, A.; Fu, Z.; Ciais, P.; Friedlingstein, P.; Sitch, S.; Pongratz, J.; Weber, U.; Reichstein, M.; Anthoni, P.; Arneth, A.; et al. Impacts of extreme summers on European ecosystems: A comparative analysis of 2003, 2010 and 2018. *Philos. Trans. R. Soc. B Biol. Sci.* **2020**, *375*, 20190507. [[CrossRef](#)]
8. Markonis, Y.; Kumar, R.; Hanel, M.; Rakovec, O.; Maca, P.; AghaKouchak, A. The rise of compound warm-season droughts in Europe. *Sci. Adv.* **2021**, *7*, eabb9668. [[CrossRef](#)]
9. Grillakis, M.G. Increase in severe and extreme soil moisture droughts for Europe under climate change. *Sci. Total Environ.* **2019**, *660*, 1245–1255. [[CrossRef](#)]
10. Samaniego, L.; Thober, S.; Kumar, R.; Wanders, N.; Rakovec, O.; Pan, M.; Zink, M.; Sheffield, J.; Wood, E.F.; Marx, A. Anthropogenic warming exacerbates European soil moisture droughts. *Nat. Clim. Chang.* **2018**, *8*, 421–426. [[CrossRef](#)]
11. Rakovec, O.; Samaniego, L.; Hari, V.; Markonis, Y.; Moravec, V.; Thober, S.; Hanel, M.; Kumar, R. The 2018–2020 Multi-Year Drought Sets a New Benchmark in Europe. *Earth's Future* **2022**, *10*, e2021EF002394. [[CrossRef](#)]
12. Naumann, G.; Cammalleri, C.; Mentaschi, L.; Feyen, L. Increased economic drought impacts in Europe with anthropogenic warming. *Nat. Clim. Chang.* **2021**, *11*, 485–491. [[CrossRef](#)]
13. Bastos, A.; Orth, R.; Reichstein, M.; Ciais, P.; Viovy, N.; Zaehle, S.; Anthoni, P.; Arneth, A.; Gentine, P.; Joetzjer, E.; et al. Vulnerability of European ecosystems to two compound dry and hot summers in 2018 and 2019. *Earth Syst. Dyn.* **2021**, *12*, 1015–1035. [[CrossRef](#)]

14. Mishra, A.K.; Singh, V.P. A review of drought concepts. *J. Hydrol.* **2010**, *391*, 202–216. [[CrossRef](#)]
15. Ramirez, A.R.; Crausbay, S.D.; Carter, S.L.; Cross, M.S.; Hall, K.R.; Bathke, D.J.; Betancourt, J.L.; Colt, S.; Cravens, A.E.; Dalton, M.S.; et al. Defining Ecological Drought for the Twenty-First Century. *Bull. Am. Meteorol. Soc.* **2017**, *98*, 2543–2550. [[CrossRef](#)]
16. van Hateren, T.C.; Chini, M.; Matgen, P.; Teuling, A.J. Ambiguous Agricultural Drought: Characterising Soil Moisture and Vegetation Droughts in Europe from Earth Observation. *Remote Sens.* **2021**, *13*, 1990. [[CrossRef](#)]
17. Keyantash, J.; Dracup, J.A. The Quantification of Drought: An Evaluation of Drought Indices. *Bull. Am. Meteorol. Soc.* **2002**, *83*, 1167–1180. [[CrossRef](#)]
18. Heim, R.R. A Review of Twentieth-Century Drought Indices Used in the United States. *Bull. Am. Meteorol. Soc.* **2002**, *83*, 1149–1166. [[CrossRef](#)]
19. Zargar, A.; Sadiq, R.; Naser, B.; Khan, F.I. A Review of Drought Indices. *Environ. Rev.* **2011**, *19*, 333–349. [[CrossRef](#)]
20. McKee, T.B.; Doesken, N.J.; Kleist, J. The relationship of drought frequency and duration to time scales. In Proceedings of the Eighth Conference on Applied Climatology, Anaheim, CA, USA, 17–22 January 1993.
21. Bachmair, S.; Tanguy, M.; Hannaford, J.; Stahl, K. How well do meteorological indicators represent agricultural and forest drought across Europe? *Environ. Res. Lett.* **2018**, *13*, 034042. [[CrossRef](#)]
22. Winkler, K.; Gessner, U.; Hochschild, V. Identifying Droughts Affecting Agriculture in Africa Based on Remote Sensing Time Series between 2000–2016: Rainfall Anomalies and Vegetation Condition in the Context of ENSO. *Remote Sens.* **2017**, *9*, 831. [[CrossRef](#)]
23. Peled, E.; Dutra, E.; Viterbo, P.; Angert, A. Technical Note: Comparing and ranking soil drought indices performance over Europe, through remote-sensing of vegetation. *Hydrol. Earth Syst. Sci.* **2010**, *14*, 271–277. [[CrossRef](#)]
24. Sepulcre-Canto, G.; Horion, S.; Singleton, A.; Carrao, H.; Vogt, J. Development of a Combined Drought Indicator to detect agricultural drought in Europe. *Nat. Hazards Earth Syst. Sci.* **2012**, *12*, 3519–3531. [[CrossRef](#)]
25. Cammalleri, C.; Arias-Muñoz, C.; Barbosa, P.; de Jager, A.; Magni, D.; Masante, D.; Mazzeschi, M.; McCormick, N.; Naumann, G.; Spinoni, J.; et al. A revision of the Combined Drought Indicator (CDI) used in the European Drought Observatory (EDO). *Nat. Hazards Earth Syst. Sci.* **2021**, *21*, 481–495. [[CrossRef](#)]
26. Vicente-Serrano, S.M.; Beguería, S.; López-Moreno, J.I. A Multiscalar Drought Index Sensitive to Global Warming: The Standardized Precipitation Evapotranspiration Index. *J. Clim.* **2010**, *23*, 1696–1718. [[CrossRef](#)]
27. Gouveia, C.M.; Trigo, R.M.; Beguería, S.; Vicente-Serrano, S.M. Drought impacts on vegetation activity in the Mediterranean region: An assessment using remote sensing data and multi-scale drought indicators. *Glob. Planet. Chang.* **2017**, *151*, 15–27. [[CrossRef](#)]
28. Vicente-Serrano, S.M.; Gouveia, C.; Camarero, J.J.; Beguería, S.; Trigo, R.; Lopez-Moreno, J.I.; Azorin-Molina, C.; Pasho, E.; Lorenzo-Lacruz, J.; Revuelto, J.; et al. Response of vegetation to drought time-scales across global land biomes. *Proc. Natl. Acad. Sci. USA* **2013**, *110*, 52–57. [[CrossRef](#)]
29. Ivits, E.; Horion, S.; Fensholt, R.; Cherlet, M. Drought footprint on European ecosystems between 1999 and 2010 assessed by remotely sensed vegetation phenology and productivity. *Glob. Chang. Biol.* **2014**, *20*, 581–593. [[CrossRef](#)]
30. Caloiero, T.; Veltri, S.; Caloiero, P.; Frustaci, F. Drought Analysis in Europe and in the Mediterranean Basin Using the Standardized Precipitation Index. *Water* **2018**, *10*, 1043. [[CrossRef](#)]
31. Palmer, W.C. *Meteorological Drought*; US Weather Bureau Research Paper; US Weather Bureau: Washington DC, USA, 1965; Volume 45.
32. Briffa, K.R.; Jones, P.D.; Hulme, M. Summer moisture variability across Europe, 1892–1991: An analysis based on the Palmer Drought Severity Index. *Int. J. Climatol.* **1994**, *14*, 475–506. [[CrossRef](#)]
33. Dabrowska-Zielinska, K.; Malinska, A.; Bochenek, Z.; Bartold, M.; Gurdak, R.; Paradowski, K.; Lagiewska, M. Drought Model DISS Based on the Fusion of Satellite and Meteorological Data under Variable Climatic Conditions. *Remote Sens.* **2020**, *12*, 2944. [[CrossRef](#)]
34. Shukla, S.; Wood, A.W. Use of a standardized runoff index for characterizing hydrologic drought. *Geophys. Res. Lett.* **2008**, *35*, L02405. [[CrossRef](#)]
35. Carrão, H.; Russo, S.; Sepulcre-Canto, G.; Barbosa, P. An empirical standardized soil moisture index for agricultural drought assessment from remotely sensed data. *Int. J. Appl. Earth Obs. Geoinf.* **2016**, *48*, 74–84. [[CrossRef](#)]
36. Martínez-Fernández, J.; González-Zamora, A.; Sánchez, N.; Gumuzzio, A.; Herrero-Jiménez, C.M. Satellite soil moisture for agricultural drought monitoring: Assessment of the SMOS derived Soil Water Deficit Index. *Remote Sens. Environ.* **2016**, *177*, 277–286. [[CrossRef](#)]
37. Kogan, F.N. Remote sensing of weather impacts on vegetation in non-homogeneous areas. *Int. J. Remote Sens.* **1989**, *11*, 1405–1419. [[CrossRef](#)]
38. Kogan, F.N. Application of Vegetation Index and Brightness Temperature for Drought Detection. *Adv. Space Res.* **1995**, *15*, 91–100. [[CrossRef](#)]
39. Hu, X.; Ren, H.; Tansey, K.; Zheng, Y.; Ghent, D.; Liu, X.; Yan, L. Agricultural drought monitoring using European Space Agency Sentinel 3A land surface temperature and normalized difference vegetation index imageries. *Agric. For. Meteorol.* **2019**, *279*, 107707. [[CrossRef](#)]
40. Buras, A.; Rammig, A.; Zang, C.S. Quantifying impacts of the 2018 drought on European ecosystems in comparison to 2003. *Biogeosciences* **2020**, *17*, 1655–1672. [[CrossRef](#)]

41. Dech, S.; Holzwarth, S.; Asam, S.; Andresen, T.; Bachmann, M.; Boettcher, M.; Dietz, A.; Eisfelder, C.; Frey, C.; Gesell, G.; et al. Challenges of Harmonizing 40 Years of AVHRR Data: The TIMELINE Experience. *Remote Sens.* **2021**, *13*, 3618. [CrossRef]
42. Reiner mann, S.; Gessner, U.; Asam, S.; Kuenzer, C.; Dech, S. The Effect of Droughts on Vegetation Condition in Germany: An Analysis Based on Two Decades of Satellite Earth Observation Time Series and Crop Yield Statistics. *Remote Sens.* **2019**, *11*, 1783. [CrossRef]
43. Gu, Y.; Brown, J.F.; Verdin, J.P.; Wardlow, B. A five-year analysis of MODIS NDVI and NDWI for grassland drought assessment over the central Great Plains of the United States. *Geophys. Res. Lett.* **2007**, *34*, L06407. [CrossRef]
44. Rossi, S.; Niemeier, S. Drought Monitoring Using Fraction of Absorbed Photosynthetically Active Radiation Estimates Derived from MERIS. In *Remote Sensing of Drought*; Wardlow, B.D., Anderson, M.C., Verdin, J.P., Eds.; CRC Press: Boca Raton, FL, USA, 2012; pp. 95–116.
45. Zscheischler, J.; Mahecha, M.D.; Harmeling, S.; Reichstein, M. Detection and attribution of large spatiotemporal extreme events in Earth observation data. *Ecol. Inform.* **2013**, *15*, 66–73. [CrossRef]
46. Panek, E.; Gozdowski, D. Relationship between MODIS Derived NDVI and Yield of Cereals for Selected European Countries. *Agronomy* **2021**, *11*, 340. [CrossRef]
47. Kloos, S.; Yuan, Y.; Castelli, M.; Menzel, A. Agricultural Drought Detection with MODIS Based Vegetation Health Indices in Southeast Germany. *Remote Sens.* **2021**, *13*, 3907. [CrossRef]
48. Lüttger, A.B.; Feike, T. Development of heat and drought related extreme weather events and their effect on winter wheat yields in Germany. *Theor. Appl. Climatol.* **2017**, *132*, 15–29. [CrossRef]
49. Möllmann, J.; Buchholz, M.; Musshoff, O. Comparing the Hedging Effectiveness of Weather Derivatives Based on Remotely Sensed Vegetation Health Indices and Meteorological Indices. *Weather. Clim. Soc.* **2019**, *11*, 33–48. [CrossRef]
50. Peichl, M.; Thober, S.; Samaniego, L.; Hansjürgens, B.; Marx, A. Climate impacts on long-term silage maize yield in Germany. *Sci. Rep.* **2019**, *9*, 7674. [CrossRef]
51. Peichl, M.; Thober, S.; Samaniego, L.; Hansjürgens, B.; Marx, A. Machine-learning methods to assess the effects of a non-linear damage spectrum taking into account soil moisture on winter wheat yields in Germany. *Hydrol. Earth Syst. Sci.* **2021**, *25*, 6523–6545. [CrossRef]
52. Liu, X.; Zheng, J.; Yu, L.; Hao, P.; Chen, B.; Xin, Q.; Fu, H.; Gong, P. Annual dynamic dataset of global cropping intensity from 2001–2019. *Sci. Data* **2021**, *8*, 283. [CrossRef]
53. Li, L.; Friedl, M.A.; Xin, Q.; Gray, J.; Pan, Y.; Froking, S. Mapping Crop Cycles in China Using MODIS-EVI Time Series. *Remote Sens.* **2014**, *6*, 2473–2493. [CrossRef]
54. Kuwata, K.; Shibasaki, R. Estimating Corn Yield in the United States with Modis Evi and Machine Learning Methods. *ISPRS Ann. Photo. Rem.* **2016**, *3*, 131–136. [CrossRef]
55. Huete, A.; Didan, K.; Miura, T.; Rodriguez, E.P.; Gao, X.; Ferreira, L.G. Overview of the radiometric and biophysical performance of the MODIS vegetation indices. *Remote Sens. Environ.* **2002**, *83*, 195–213. [CrossRef]
56. DWD. *German Climate Atlas*; DWD: Offenbach, Germany, 2023. Available online: https://www.dwd.de/EN/climate_environment/climateatlas/climateatlas_node.html (accessed on 1 September 2023).
57. Destatis. Land- und Forstwirtschaft, Fischerei. Feldfrüchte und Grünland. Available online: https://www.destatis.de/DE/Themen/Branchen-Unternehmen/Landwirtschaft-Forstwirtschaft-Fischerei/Feldfruechte-Gruenland/_inhalt.html (accessed on 1 September 2023).
58. Destatis. *Genesis. Die Datenbank des Statistischen Bundesamtes*; Destatis: Wiesbaden, Germany, 2023. Available online: <https://www-genesis.destatis.de/genesis/online> (accessed on 1 September 2023).
59. DWD Climate Data Center (CDC). *Multi-Annual Means of Grids of Air Temperature (2m) over Germany 1921–2020*; DWD Climate Data Center (CDC): Offenbach, Germany, 2021. Available online: https://opendata.dwd.de/climate_environment/CDC/grids_germany/multi_annual/air_temperature_mean/ (accessed on 1 September 2023).
60. DWD Climate Data Center (CDC). *Multi-Annual Means of Grids of Monthly Averaged Daily Maximum Air Temperature (2m) over Germany 1991–2020, Version v1.0*; DWD Climate Data Center (CDC): Offenbach, Germany, 2021. Available online: https://opendata.dwd.de/climate_environment/CDC/grids_germany/multi_annual/air_temperature_max/ (accessed on 1 September 2023).
61. DWD Climate Data Center (CDC). *Multi-Annual Grids of Precipitation Height over GERMANY 1991–2020, Version v1.0*; DWD Climate Data Center (CDC): Offenbach, Germany, 2021. Available online: https://opendata.dwd.de/climate_environment/CDC/grids_germany/multi_annual/precipitation/ (accessed on 1 September 2023).
62. Bundesanstalt für Geowissenschaften und Rohstoffe. *Ackerbauliches Ertragspotential der Böden in Deutschland 1:1.000.000*; Bundesanstalt für Geowissenschaften und Rohstoffe: Hanover, Germany, 2020.
63. Müller, L.; Schindler, U.; Behrendt, A.; Eulenstein, F.; Dannowski, R. *The Müncheberg Soil Quality Rating. Field Manual for Detecting and Assessing Properties and Limitations of Soils for Cropping and Grazing*; Leibniz-Zentrum für Agrarlandschaftsforschung (ZALF): Müncheberg, Germany, 2007.
64. European Union’s Copernicus Land Monitoring Service. *CORINE Land Cover 2018*. European Environment Agency: Copenhagen, Denmark, 2019. [CrossRef]
65. DWD. *Klimastatusbericht Deutschland Jahr 2022*; DWD: Offenbach, Germany, 2023; p. 27. Available online: https://www.dwd.de/DE/leistungen/klimastatusbericht/publikationen/ksb_2022.pdf?__blob=publicationFile&v=5 (accessed on 1 September 2023).

66. DWD. *Klimastatusbericht Deutschland Jahr 2021*; DWD: Offenbach, Germany, 2022; p. 27. Available online: https://www.dwd.de/DE/leistungen/klimastatusbericht/publikationen/ksb_2021.pdf?__blob=publicationFile&v=4 (accessed on 1 September 2023).
67. DWD. *Klimastatusbericht Deutschland Jahr 2018*; DWD: Offenbach, Germany, 2020; p. 23. Available online: https://www.dwd.de/DE/leistungen/klimastatusbericht/publikationen/ksb_2018.pdf?__blob=publicationFile&v=5 (accessed on 1 September 2023).
68. DWD. *Klimastatusbericht Deutschland Jahr 2019*; DWD: Offenbach, Germany, 2020; p. 23. Available online: https://www.dwd.de/DE/leistungen/klimastatusbericht/publikationen/ksb_2019.pdf?__blob=publicationFile&v=5 (accessed on 1 September 2023).
69. DWD. *Klimastatusbericht Deutschland Jahr 2020*; DWD: Offenbach, Germany, 2021; p. 29. Available online: https://www.dwd.de/DE/leistungen/klimastatusbericht/publikationen/ksb_2020.pdf?__blob=publicationFile&v=3 (accessed on 1 September 2023).
70. BMEL. Besondere Ernte- und Qualitätsermittlung (BEE) 2021; 0178—899 X. 2022, p. 70. Available online: <https://www.bmel-statistik.de/fileadmin/daten/1002000-2021.pdf> (accessed on 1 September 2023).
71. Destatis. *Land- und Forstwirtschaft, Fischerei. Wachstum und Ernte—Feldfrüchte—August/September 2022*; Destatis: Wiesbaden, Germany, 2022; p. 78. Available online: https://www.statistischebibliothek.de/mir/servlets/MCRFileNodeServlet/DEHeft_derivate_00071981/2030321222094.pdf (accessed on 1 September 2023).
72. Didan, K. MODIS/Terra Vegetation Indices 16-Day L3 Global 250m SIN Grid V061. 2021, Distributed by NASA EOSDIS Land Processes Distributed Active Archive Center. Available online: <https://ladsweb.modaps.eosdis.nasa.gov/missions-and-measurements/products/MOD13Q1> (accessed on 10 October 2023).
73. European Union's Copernicus Land Monitoring Service. *CORINE Land Cover*; European Environment Agency: Copenhagen, Denmark. Available online: <https://land.copernicus.eu/en/products/corine-land-cover> (accessed on 1 September 2023).
74. Destatis. Land- und Forstwirtschaft, Fischerei. In *Wachstum und Ernte—Feldfrüchte*; Destatis: Wiesbaden, Germany, 2022. Available online: https://www.destatis.de/DE/Themen/Branchen-Unternehmen/Landwirtschaft-Forstwirtschaft-Fischerei/Feldfruechte-Gruenland/Publikationen/Downloads-Feldfruechte/feldfruechte-jahr-2030321227164.pdf?__blob=publicationFile (accessed on 1 September 2023).
75. Ernte- und Betriebsberichterstattungen (EBE). Erträge Ausgewählter Landwirtschaftlicher Feldfrüchte-. Available online: https://www.statistischebibliothek.de/mir/servlets/MCRFileNodeServlet/DEMografie_derivate_00001133/ErnteEBE.pdf;jsessionid=F1F65AD17A67F615151ED405D4C5B2F9 (accessed on 1 October 2023).
76. Jahressumme—Regionale Tiefe: Kreise und krfr. Städte. Regionaldatenbank Deutschland (RDB). Statistische Ämter des Bundes und der Länder. Available online: <https://www.regionalstatistik.de/genesis/online/> (accessed on 1 September 2023).
77. Destatis. *Qualitätsbericht Ernte- und Betriebsberichterstattung (EBE): Feldfrüchte und Grünland*; Destatis: Wiesbaden, Germany, 2023. Available online: https://www.destatis.de/DE/Methoden/Qualitaet/Qualitaetsberichte/Land-Forstwirtschaft-Fischerei/ernte-ebe.pdf?__blob=publicationFile (accessed on 1 September 2023).
78. Gorelick, N.; Hancher, M.; Dixon, M.; Ilyushchenko, S.; Thau, D.; Moore, R. Google Earth Engine: Planetary-scale geospatial analysis for everyone. *Remote Sens. Environ.* **2017**, *202*, 18–27. [CrossRef]
79. UFZ. Dürren in Deutschland. Available online: <https://www.ufz.de/index.php?de=47252> (accessed on 1 September 2023).
80. Steduto, P.; Hsiao, T.C.; Fereres, E.; Raes, D. *Crop Yield Response to Water*; FAO: Rome, Italy, 2012.
81. Monteleone, B.; Borzì, I.; Bonaccorso, B.; Martina, M. Developing stage-specific drought vulnerability curves for maize: The case study of the Po River basin. *Agric. Water Manag.* **2022**, *269*, 107713. [CrossRef]
82. Riedesel, L.; Moller, M.; Horney, P.; Golla, B.; Piepho, H.P.; Kautz, T.; Feike, T. Timing and intensity of heat and drought stress determine wheat yield losses in Germany. *PLoS ONE* **2023**, *18*, e0288202. [CrossRef] [PubMed]
83. Sarto, M.V.M.; Sarto, J.R.W.; Rampim, L.; Rosset, J.S.; Bassegio, D.; da Costa, P.F.; Inagaki, A.M. Wheat phenology and yield under drought: A review. *Aust. J. Crop Sci.* **2017**, *11*, 941–946. [CrossRef]
84. Radočaj, D.; Šiljeg, A.; Marinović, R.; Jurišić, M. State of Major Vegetation Indices in Precision Agriculture Studies Indexed in Web of Science: A Review. *Agriculture* **2023**, *13*, 707. [CrossRef]
85. Reinermann, S.; Gessner, U.; Asam, S.; Ullmann, T.; Schucknecht, A.; Kuenzer, C. Detection of grassland mowing events for Germany by combining Sentinel-1 and Sentinel-2 time series. *Remote Sens.* **2022**, *14*, 1647. [CrossRef]
86. Schwieder, M.; Wesemeyer, M.; Frantz, D.; Pfoch, K.; Erasmi, S.; Pickert, J.; Nendel, C.; Hostert, P. Mapping grassland mowing events across Germany based on combined Sentinel-2 and Landsat 8 time series. *Remote Sens. Environ.* **2022**, *269*, 112795. [CrossRef]
87. Wu, M.; Manzoni, S.; Vico, G.; Bastos, A.; de Vries, F.T.; Messori, G. Drought Legacy in Sub-Seasonal Vegetation State and Sensitivity to Climate Over the Northern Hemisphere. *Geophys. Res. Lett.* **2022**, *49*, e2022GL098700. [CrossRef]
88. Seidel, P. Extreme weather events and their effects on plant pests infesting wheat, barley and maize. *J. Fur Kult.* **2016**, *68*, 313–327. [CrossRef]
89. Seidel, P. Extreme weather events and their effects on plant pests infecting potato, sugar beet, rape and grassland. *J. Fur Kult.* **2017**, *69*, 125–136. [CrossRef]
90. Glenn, E.P.; Huete, A.R.; Nagler, P.L.; Nelson, S.G. Relationship Between Remotely-sensed Vegetation Indices, Canopy Attributes and Plant Physiological Processes: What Vegetation Indices Can and Cannot Tell Us About the Landscape. *Sensors* **2008**, *8*, 2136–2160. [CrossRef] [PubMed]

91. Didan, K.; Munoz, A.B.; Comptom, T.J.; Pinzon, J.E. Suomi National Polar-orbiting Partnership Visible Infrared Imaging Radiometer Suite Vegetation Index Product Suite User Guide & Abridged Algorithm Theoretical Basis Document Version 2.0. 2017. Available online: https://viirsland.gsfc.nasa.gov/PDF/SNPP_VIIRS_VI_UserGuide_09-26-2017_KDidan.pdf (accessed on 1 September 2023).
92. Jarchow, C.J.; Didan, K.; Barreto-Munoz, A.; Nagler, P.L.; Glenn, E.P. Application and Comparison of the MODIS-Derived Enhanced Vegetation Index to VIIRS, Landsat 5 TM and Landsat 8 OLI Platforms: A Case Study in the Arid Colorado River Delta, Mexico. *Sensors* **2018**, *18*, 1546. [[CrossRef](#)] [[PubMed](#)]
93. Obata, K.; Miura, T.; Yoshioka, H.; Huete, A.R.; Vargas, M. Spectral Cross-Calibration of VIIRS Enhanced Vegetation Index with MODIS: A Case Study Using Year-Long Global Data. *Remote Sens.* **2016**, *8*, 34. [[CrossRef](#)]
94. Uereyen, S.; Bachofer, F.; Kuenzer, C. A Framework for Multivariate Analysis of Land Surface Dynamics and Driving Variables—A Case Study for Indo-Gangetic River Basins. *Remote Sens.* **2022**, *14*, 197. [[CrossRef](#)]
95. Chen, T.; Guestrin, C. XGBoost: A Scalable Tree Boosting System. In Proceedings of the 22nd ACM SIGKDD International Conference on Knowledge Discovery and Data Mining, San Francisco, CA, USA, 13–17 August 2016; pp. 785–794.
96. Bartold, M.; Kluczek, M. A Machine Learning Approach for Mapping Chlorophyll Fluorescence at Inland Wetlands. *Remote Sens.* **2023**, *15*, 2392. [[CrossRef](#)]
97. Friedman, J.H. Stochastic gradient boosting. *Comput. Stat. Data Anal.* **2002**, *38*, 367–378. [[CrossRef](#)]

Disclaimer/Publisher’s Note: The statements, opinions and data contained in all publications are solely those of the individual author(s) and contributor(s) and not of MDPI and/or the editor(s). MDPI and/or the editor(s) disclaim responsibility for any injury to people or property resulting from any ideas, methods, instructions or products referred to in the content.